

# OBSERVATIONS AND MODELING OF INTERNAL WAVES IN THE SHELF ZONE OF THE JAPAN/EAST SEA

V.V.Navrotsky, V.Yu. Liapidevskii, E.P.Pavlova

**POI FEB RAS**

**LIH SB RAS**

[navrotskyv@poi.dvo.ru](mailto:navrotskyv@poi.dvo.ru)

[liapid@hydro.nsc.ru](mailto:liapid@hydro.nsc.ru)

[pavlova@poi.dvo.ru](mailto:pavlova@poi.dvo.ru)

# CONTENTS

- General: energy and structure considerations
- Observations of internal waves in the coastal ocean
- Modeling of internal wave generation and propagation in the shelf zone
- Consequences:
  - a) diffusion amplification
  - b) fine structure formation
  - c) nonlinear fluxes to higher modes, thermocline splitting, and layering of vertical structure – positive feedback

Internal waves on a sloping bottom

Experiments in the Japanese/East sea

# Observations of internal waves in the coastal ocean

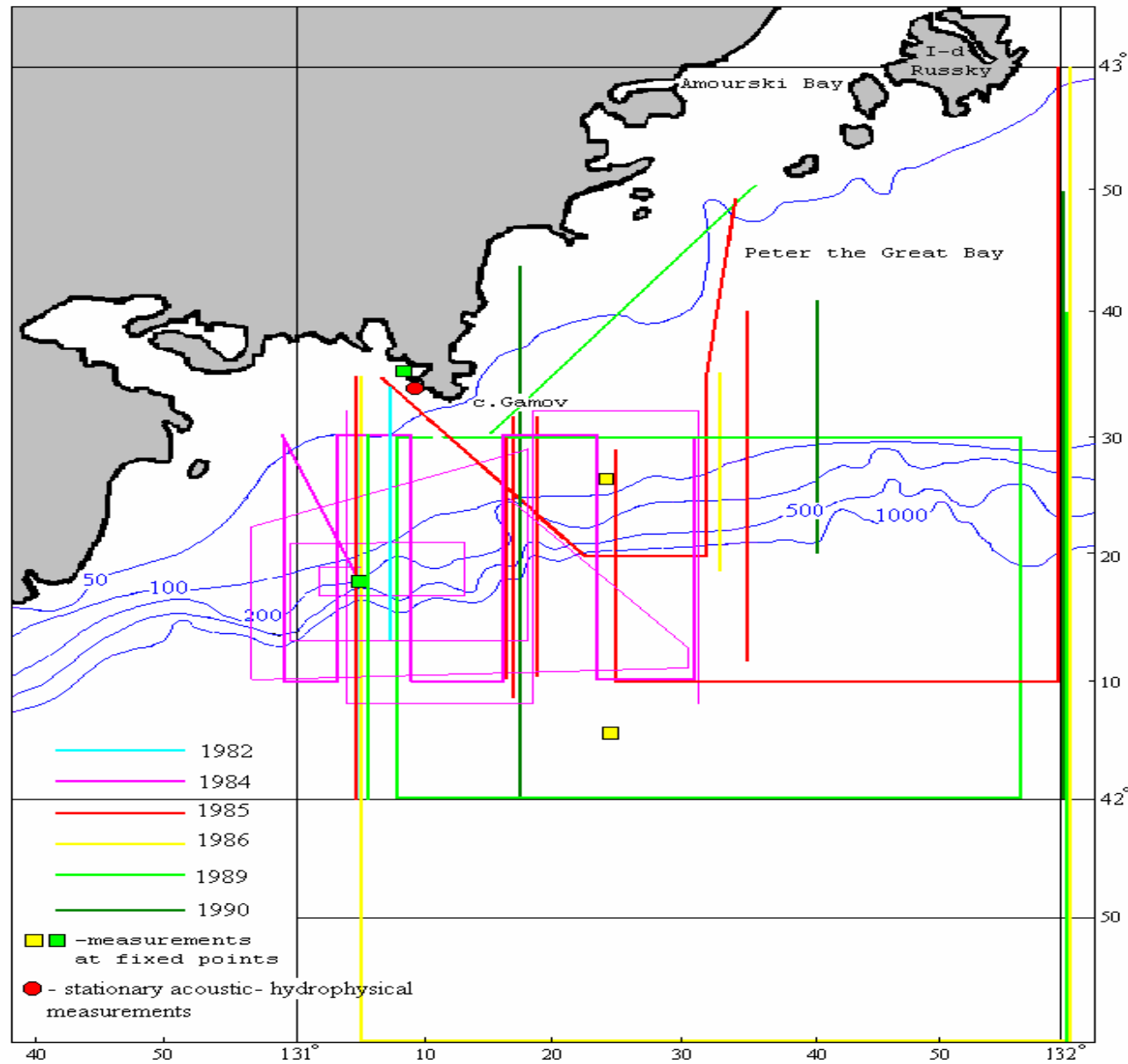
- Temporal fluctuations – examples Jap. Sea, Australian shelf (Holloway)
- Spatial fluctuations – transects with linear sensors

# General view of the geophysical measurement site



# Region of observations

Scheme of works in the Japanese Sea



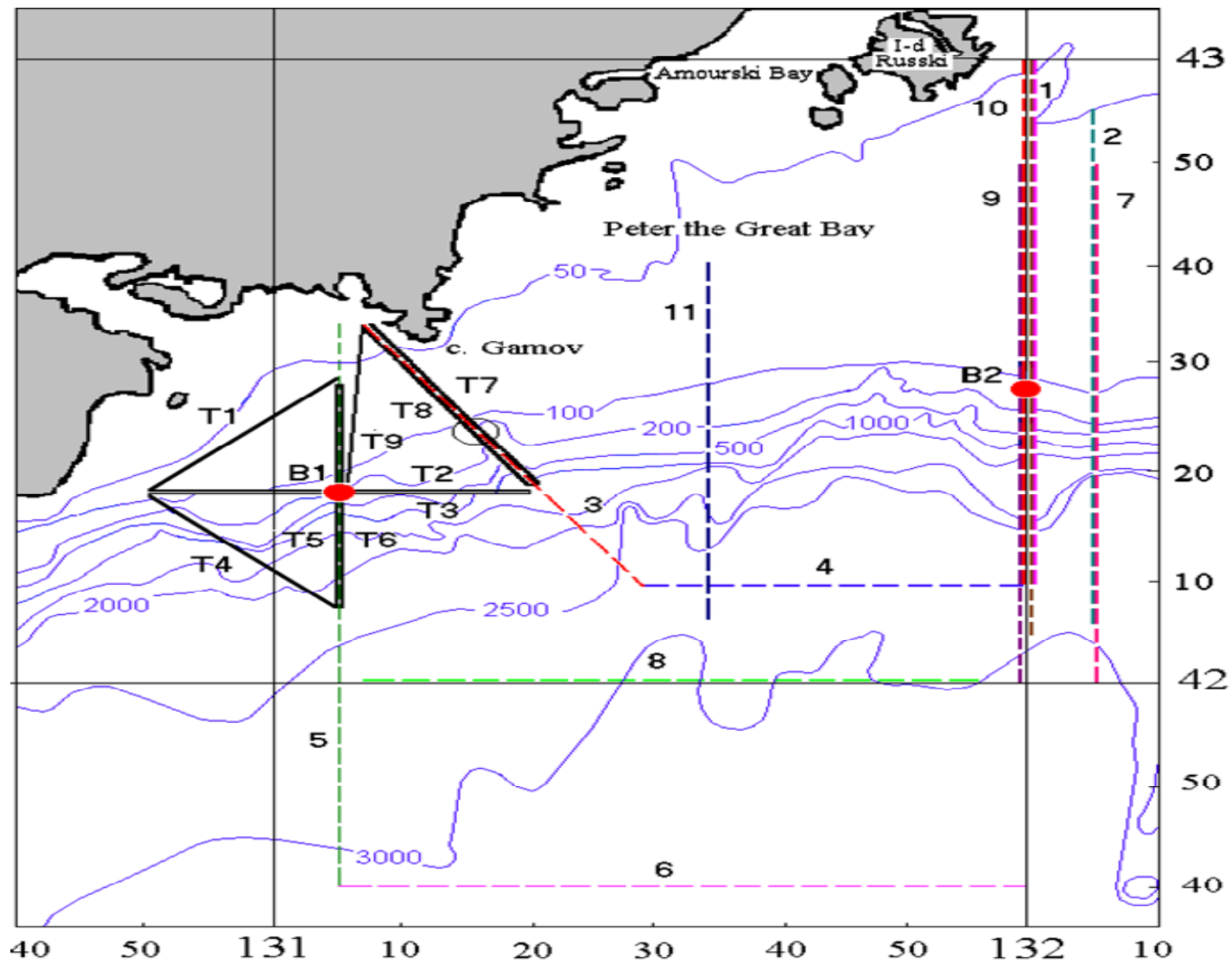
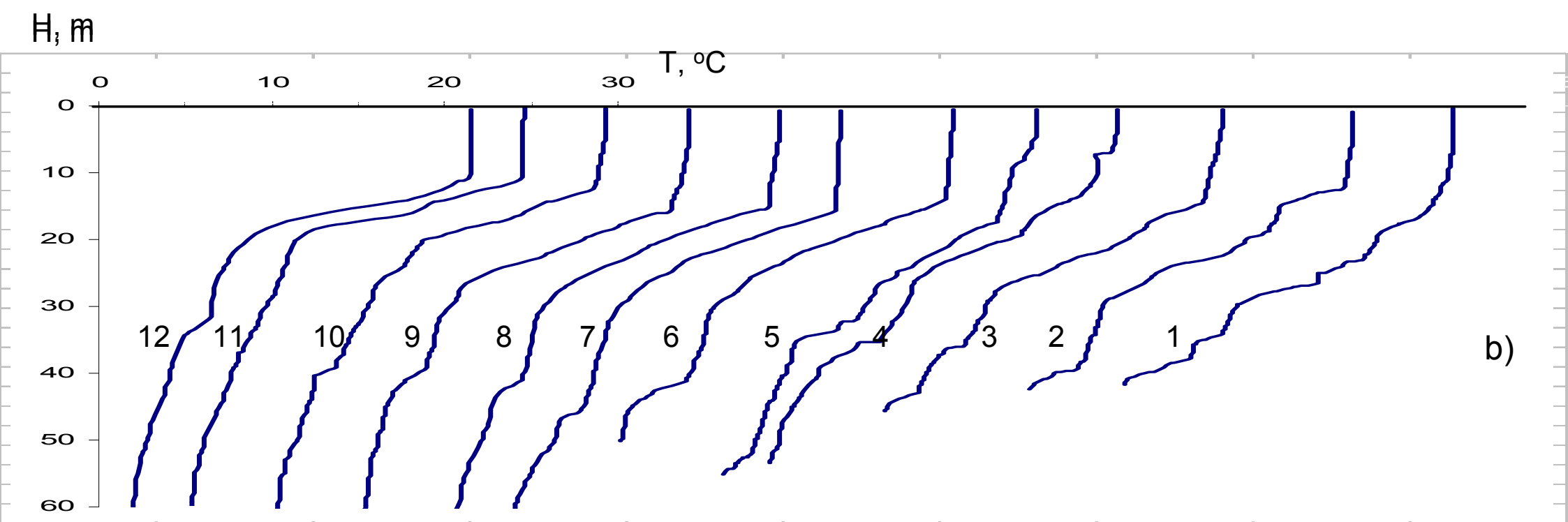
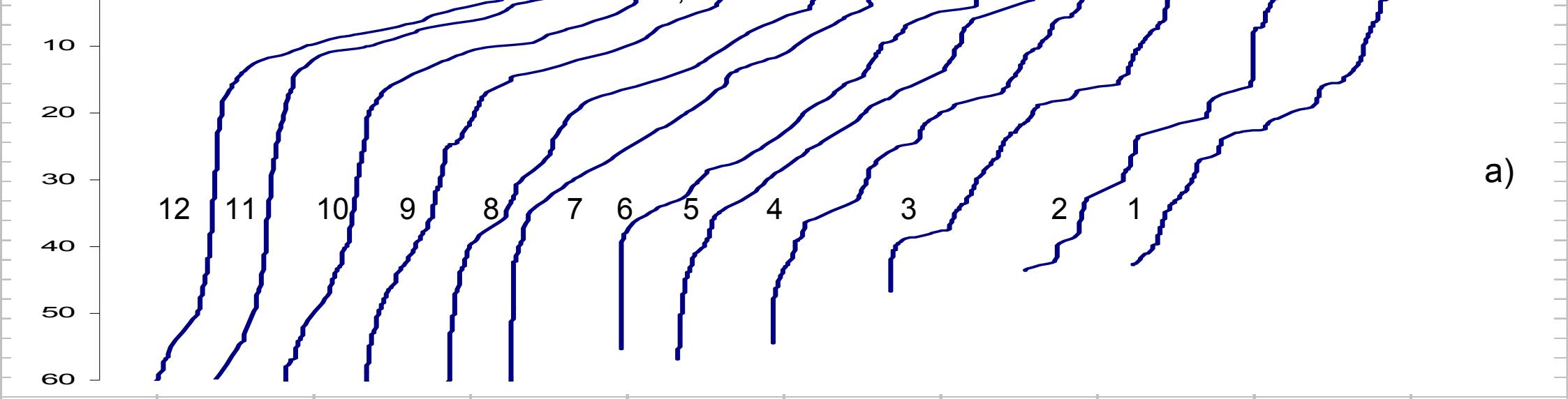


Fig. 1. The study region. Dotted lines for runs with CTD-probing, solid lines for runs with towed sensors. Black circles show locations of the stations where observations during 1-3 days were made.



**Temperature profiles along transects across the shelf boundary: 12.08.2006**



Fig. 2. Internal wave records in fixed points: a) Point B1 (start at 19:30, 05.09.1984);  
 b) Point B2 (start at 13:24, 28.09.1986).

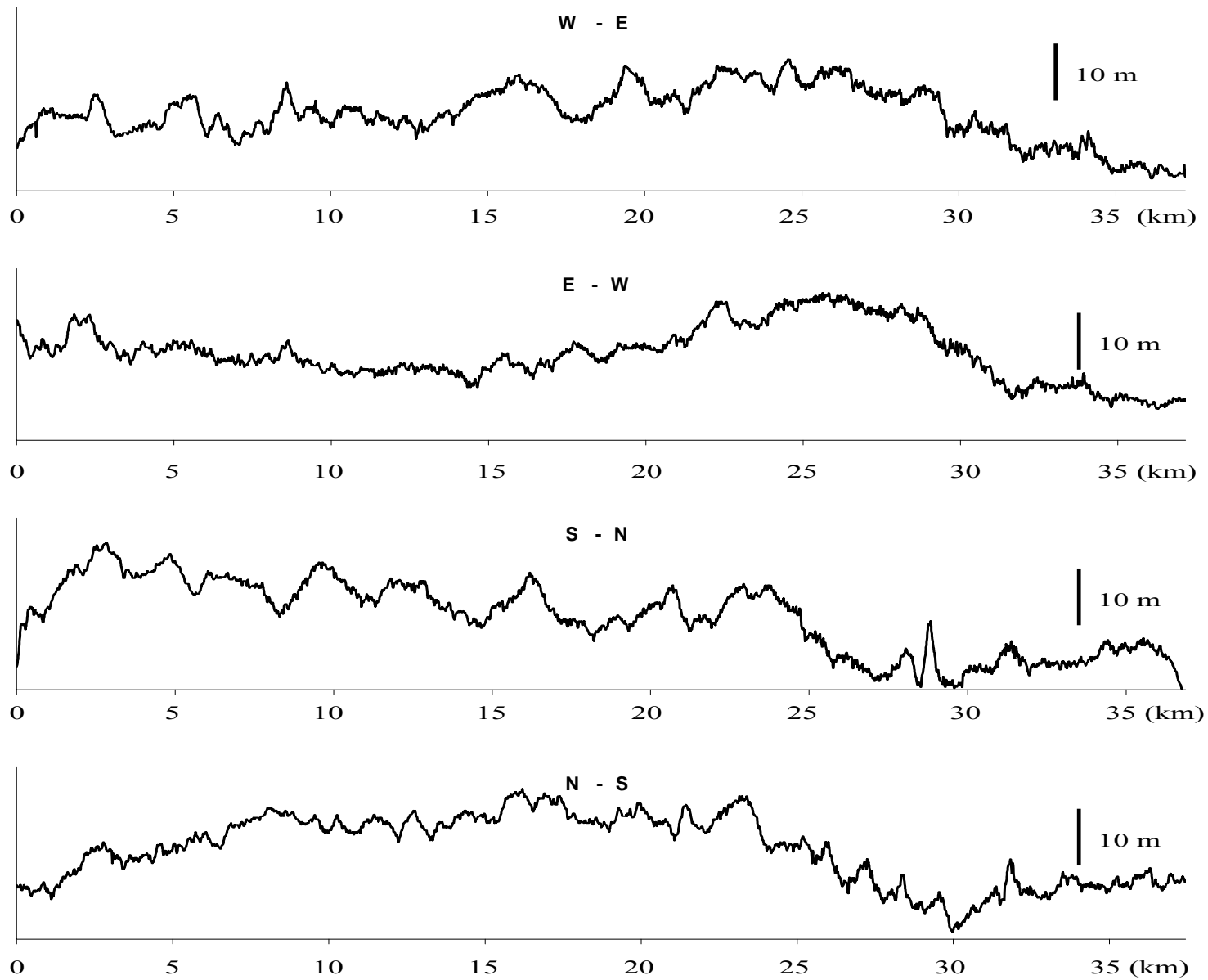


Fig. 3. Vertical movements in the thermocline, obtained with the help of the towed line sensor on crossing runs (see Fig. 1).

## b) Thermocline splitting, fine structure formation

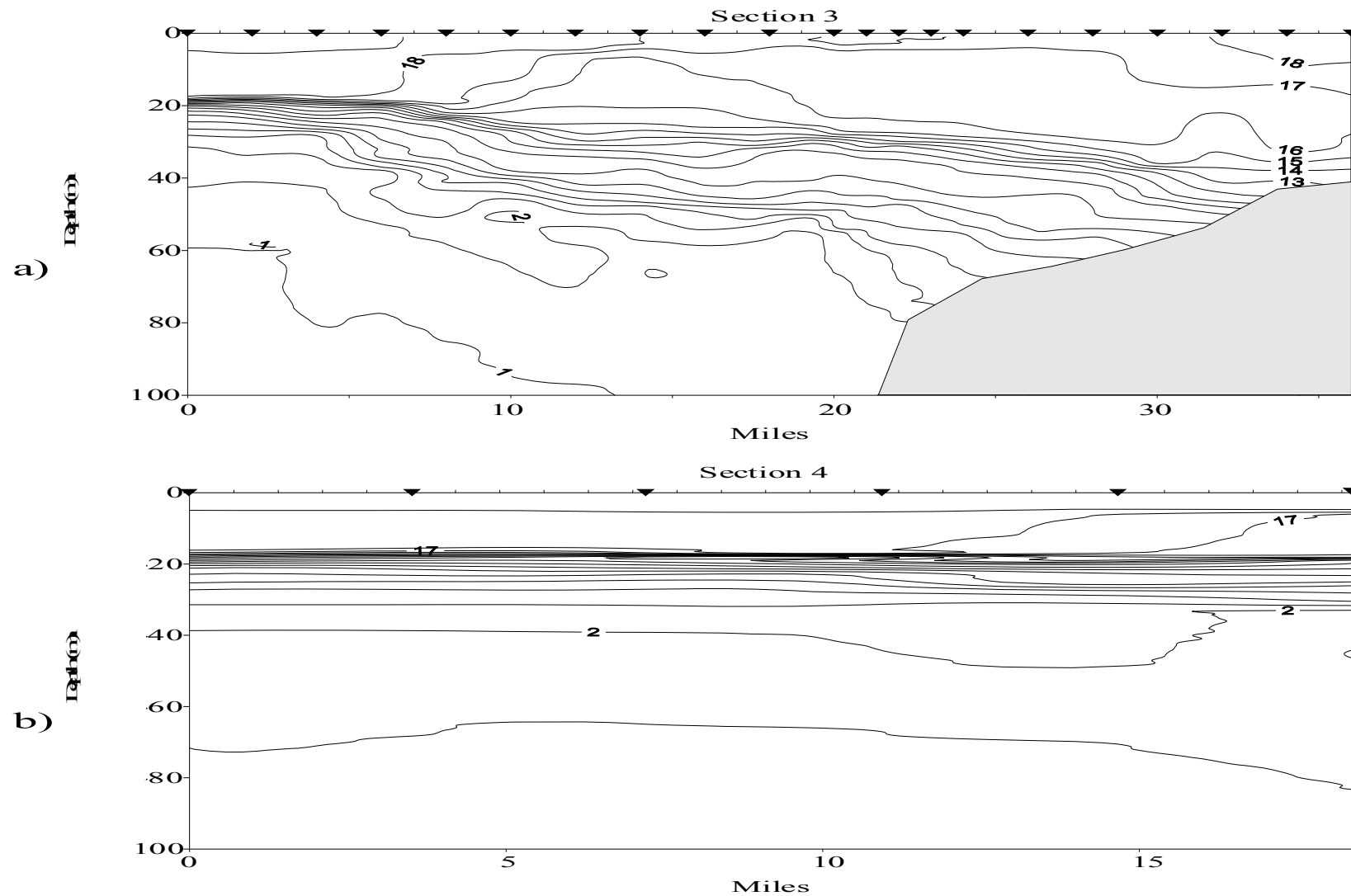


Fig. 5. Sections of temperature:  
a) across isobaths, 22. 07.1985, along run 3;  
b) along isobaths, 23.07.1985, along  $42^{\circ} 10' N$ .

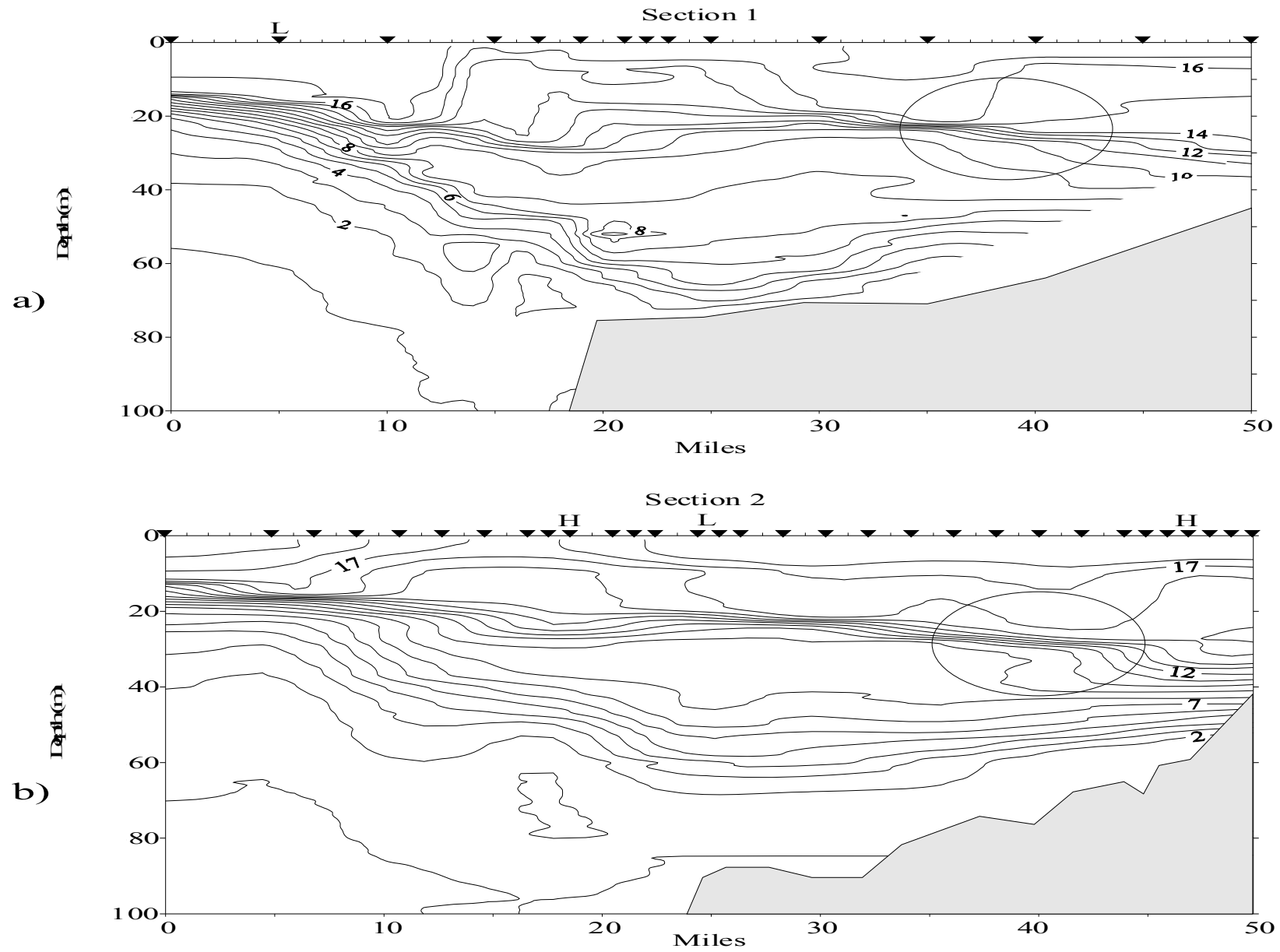


Fig. 4. Section of temperature distribution along transects across the slope and shelf boundary: a) 13-14. 07.1985; b) 15-16.07.1985. Triangles mark position of the stations with CTD-probing.

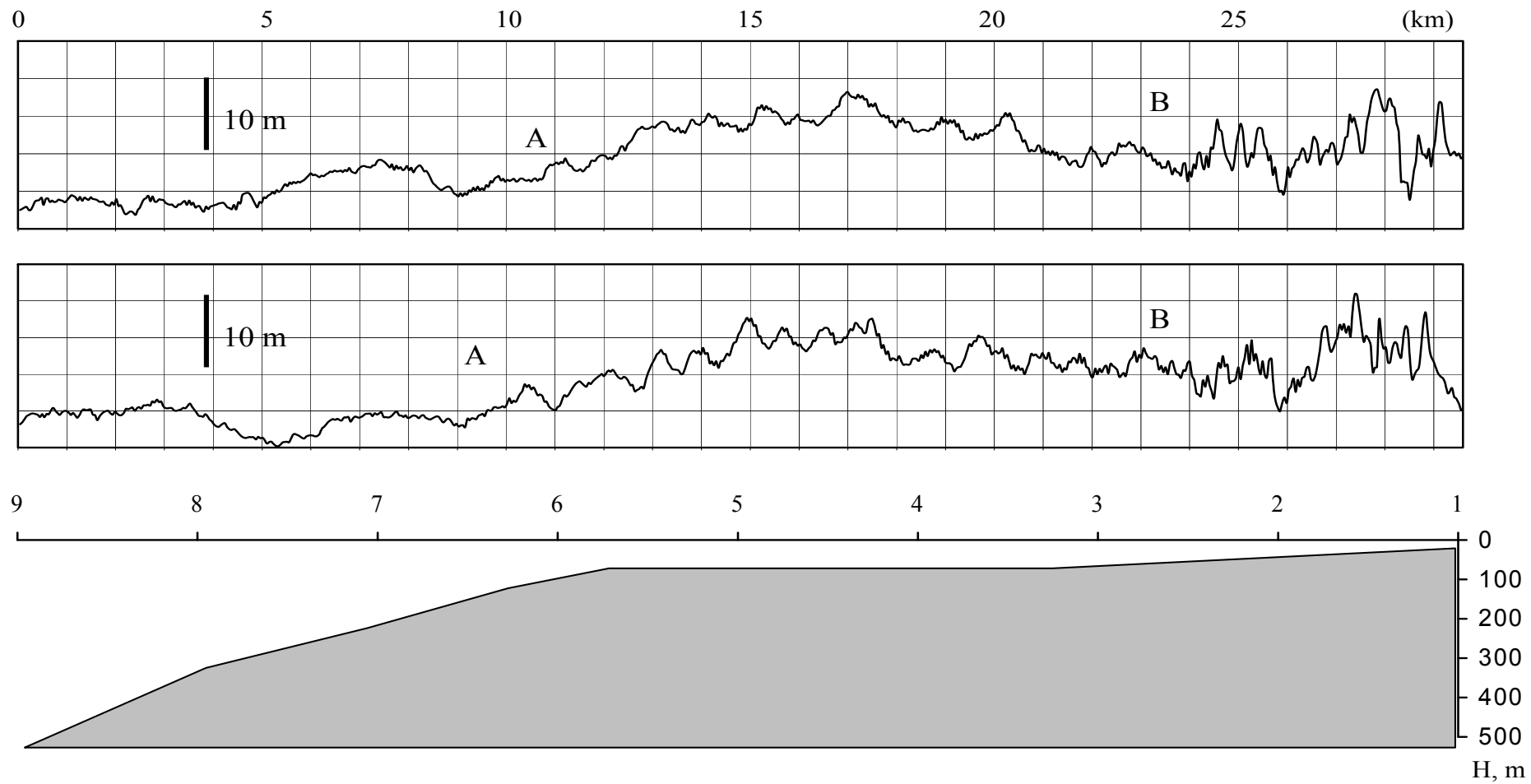


Fig. 4. Offshore and onshore runs across shelf and shelf break, 23.09.1984. Numbers 1-9 mark positions of the stations with CTD-probing.

# Models of internal wave generation and propagation in the shelf zone

- Equations and calculations
  - Generation near the shelf break
- Propagation and transformation - ACD

# Equations

$$(U + W_1)_\tau + \left(\frac{1}{2}U^2 + gZ + W_2\right)_\xi + \frac{P_\xi}{\rho} - \frac{1}{\rho^2} \overline{\rho' k p'_\theta} = \frac{1}{\rho} \left[ \mu(U_\eta + W_3) \right]_\eta - \nu W_4 \quad (1)$$

$$\rho C(T_\tau + UT_\xi) = \left[ \lambda \left( 1 + \overline{z'_\eta{}^2} + k^2 \overline{z'_\theta{}^2} \right) T_\eta \right]_\eta \quad (2)$$

$$S_\tau + [U(1 - S)]_\xi = 0 \quad (3)$$

$$P_\eta = -\rho g \quad (4)$$

$$\rho(1 + Z_\zeta) = \rho_0(1 - S) \quad (5)$$

$$\rho(U - c)^2 k^2 z'_{\theta\theta} + \rho g z'_\eta + p'_\eta = 0,$$

$$p' = \rho(U - c)^2 z'_\eta - \rho g z', \quad (6)$$

$$\rho C(U - c)(kt'_\theta - T_\xi z'_\eta)' = -2(\lambda T_\eta)_\eta z'_\eta - \lambda T_\eta (z'_{\eta\eta} + k^2 z'_{\theta\theta}) \quad (7)$$

$$\begin{aligned} & \left[ \int \rho k^{-1} W_1 d\eta \right]_\tau + \left[ \int \rho k^{-1} (U - c) (c \overline{z'^2_\eta} + U k^2 \overline{z'^2_\theta}) d\eta \right]_\xi - \int \rho^{-1} \overline{\rho' p'_\theta} d\eta = \\ & - \int \mu k^{-1} W_4 d\eta + \delta \left\{ \mu k^{-1} \left[ \frac{1}{2} (U - c) (\overline{z'^2_\eta} + k^2 \overline{z'^2_\theta})_\eta + U_\eta (3 \overline{z'^2_\eta} + k^2 \overline{z'^2_\theta}) \right] \right\} \end{aligned} \quad (8)$$

$\xi, \zeta, \tau$  – horizontal Euler coordinate, vertical Lagrange coordinate and time,  
 $T, U$  и  $S$  – mean temperature of a layer, Lagrange mean horizontal velocity  
 and mean deformation coefficient of a layer,  $1-S$  – horizontal compression  
 of fluid element relative to the standard state, “layer” means the aggregate of  
 fluid particles having the same Lagrange coordinate,  
 $\rho_0$  – standard density,

$$W_1 = (U - c) \left( \overline{z'_\eta{}^2} + k^2 \overline{z'_\theta{}^2} \right)$$

$$W_2 = UW_1 + \frac{1}{2} (U - c)^2 \left( \overline{z'_\eta{}^2} - k^2 \overline{z'_\theta{}^2} \right)$$

$$\mu W_3 = \mu \left[ U_\eta \left( 6 \overline{z'_\eta{}^2} + 2k^2 \overline{z'_\theta{}^2} \right) + (U - c) \left( 2 \overline{z'_\eta{}^2} + k^2 \overline{z'_\theta{}^2} \right)_\eta \right]$$

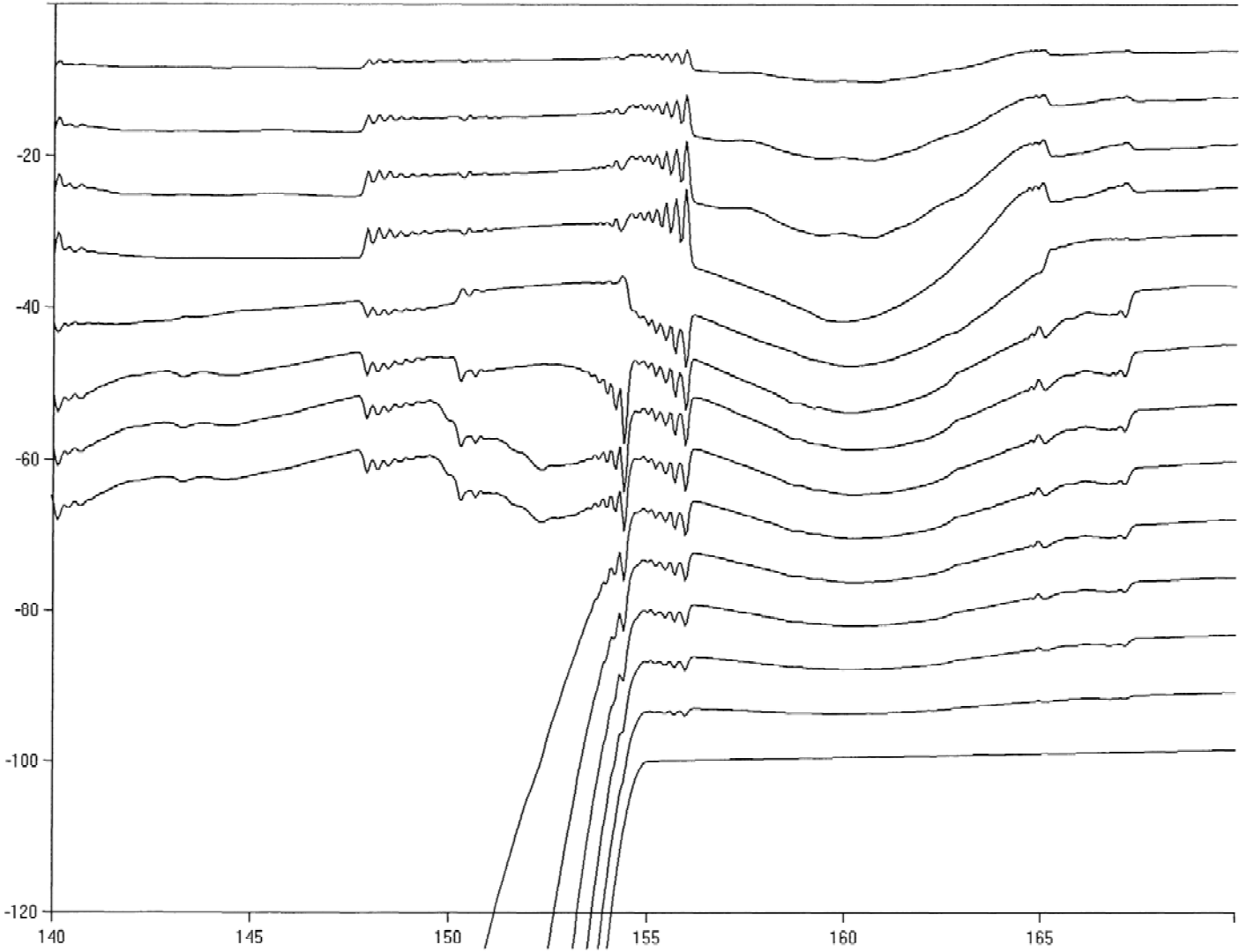
$$-v W_4 = -v \left[ 2U_\eta \left( k^2 \overline{z'_\theta{}^2} + \overline{z'_\eta{}^2} \right)_\eta + (U - c) \left( k^4 \overline{z'_{\theta\theta}{}^2} + 2k^2 \overline{z'_{\theta\eta}{}^2} + \overline{z'_{\eta\eta}{}^2} \right) \right]$$

$$\eta = \zeta + Z,$$

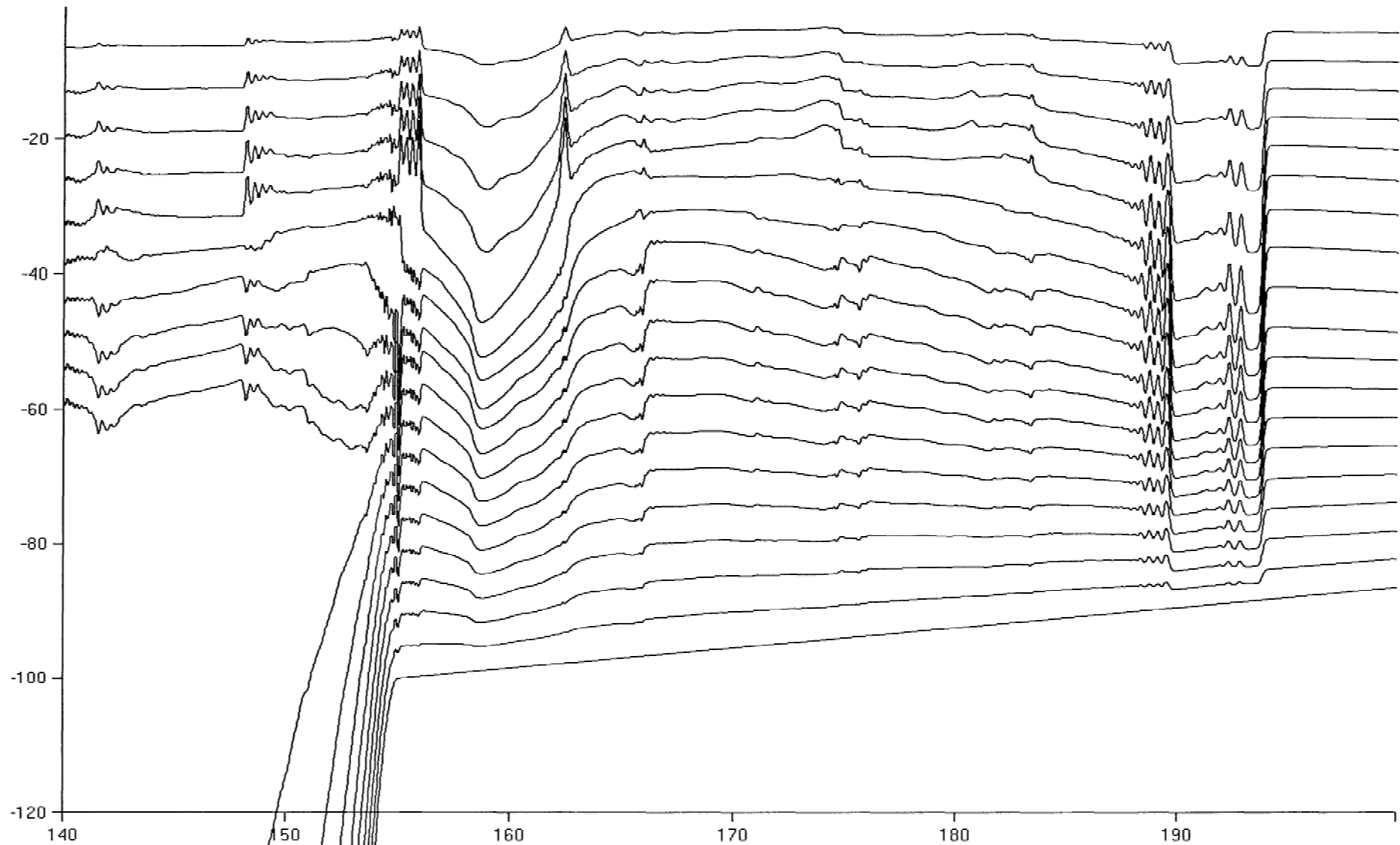
$$\theta_\xi = k$$

$$c = -\theta_\tau / k$$

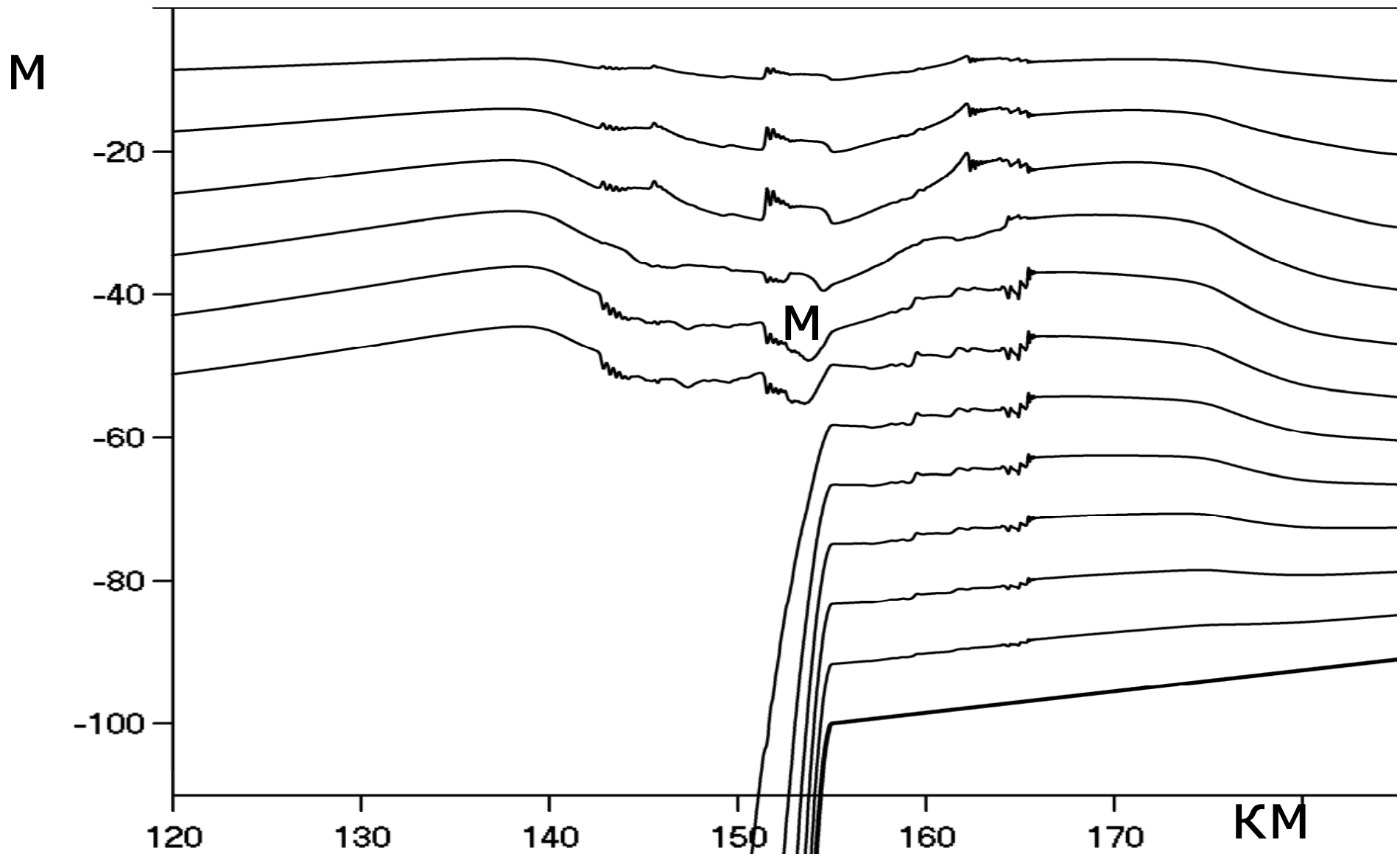
Near the ShB,  $\nu = 0.4 \text{ m/s}$ , horiz visc = 1 sqm/s. Second mode formation



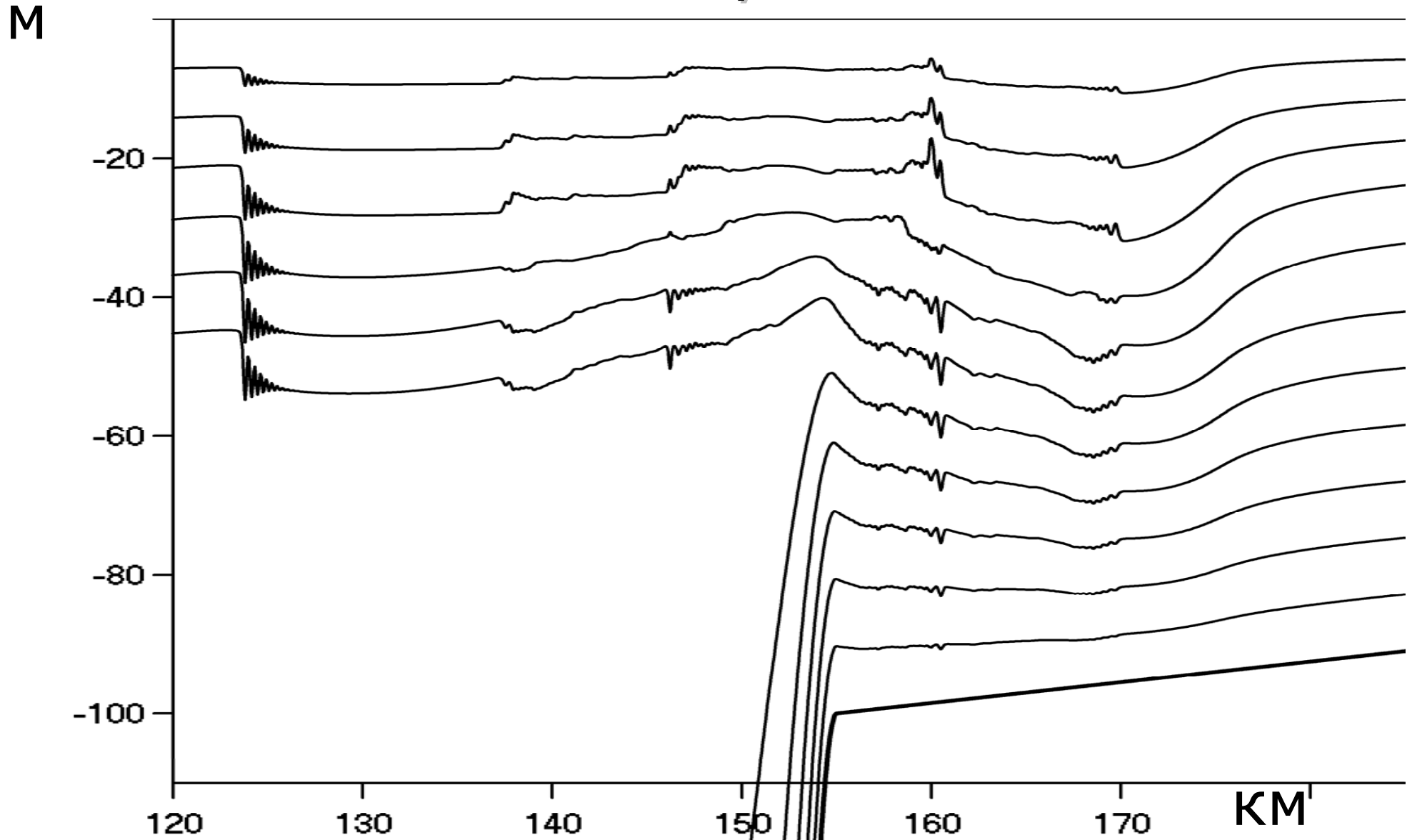
$\nu = 0.5 \text{ m/s}$ ,  $\text{vert visc} = 0.002 \text{ sqm/s}$ . Jumps formation



# Maximum of internal tide 21 h after the start of 12-h surface tide from initial 0-velocity state

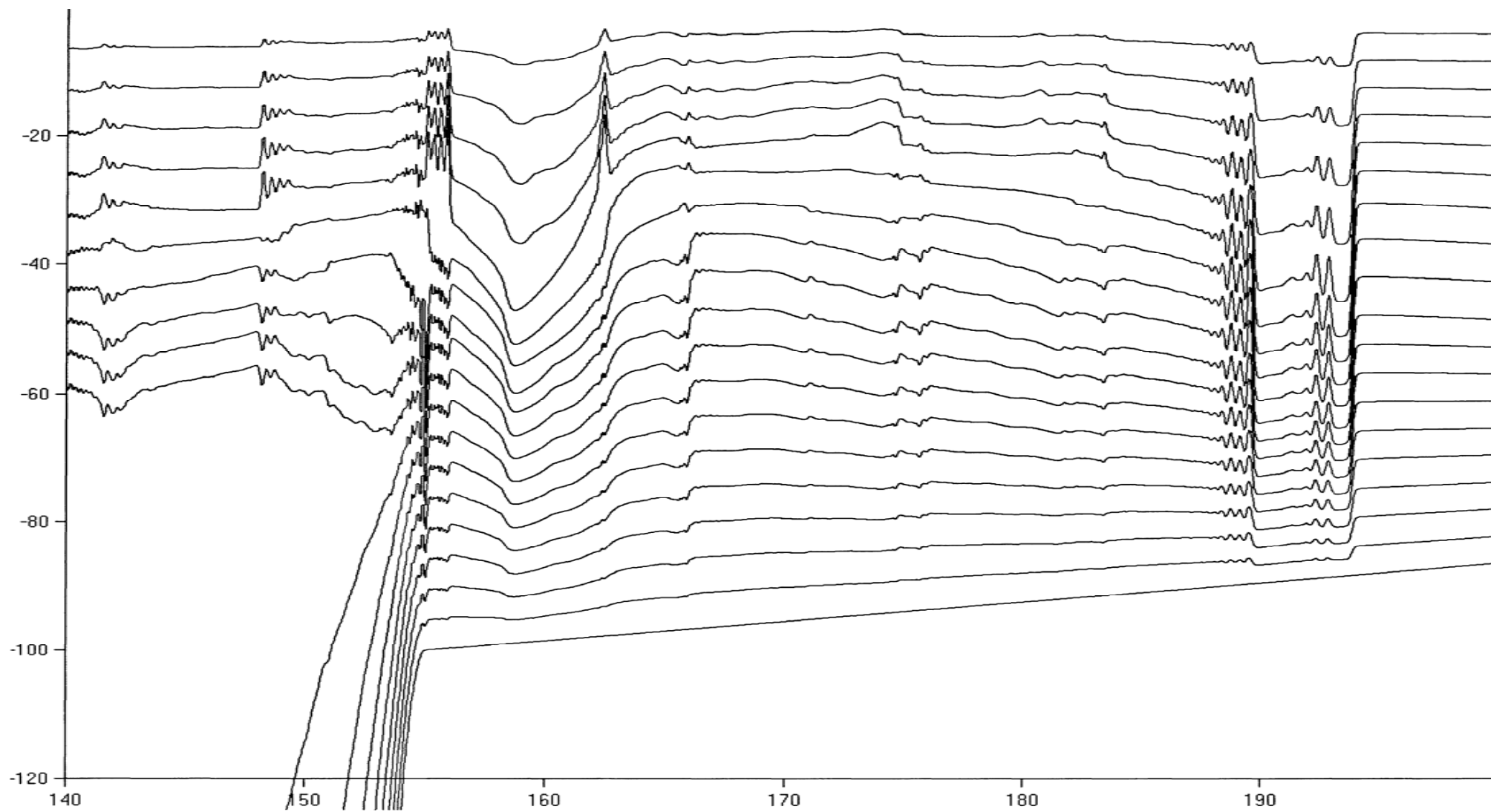


# Minimum of internal tide 27 h after the start of 12-h surface tide from initial 0-velocity state



# More detailed results

- 15-2, 24-3,4 – FXT
- Sel 0 (ACD) - generation
- Sel 48 (ACD) - propagation and transformation



- Generation near the shelf break –  
ACDSee – Sel-0
- Propagation and transformation - ACDSee  
– Sel-
- 15-2 & 24-3,4 – two steps (Nmax) – ACD?

# Consequencies: a) diffusion amplification

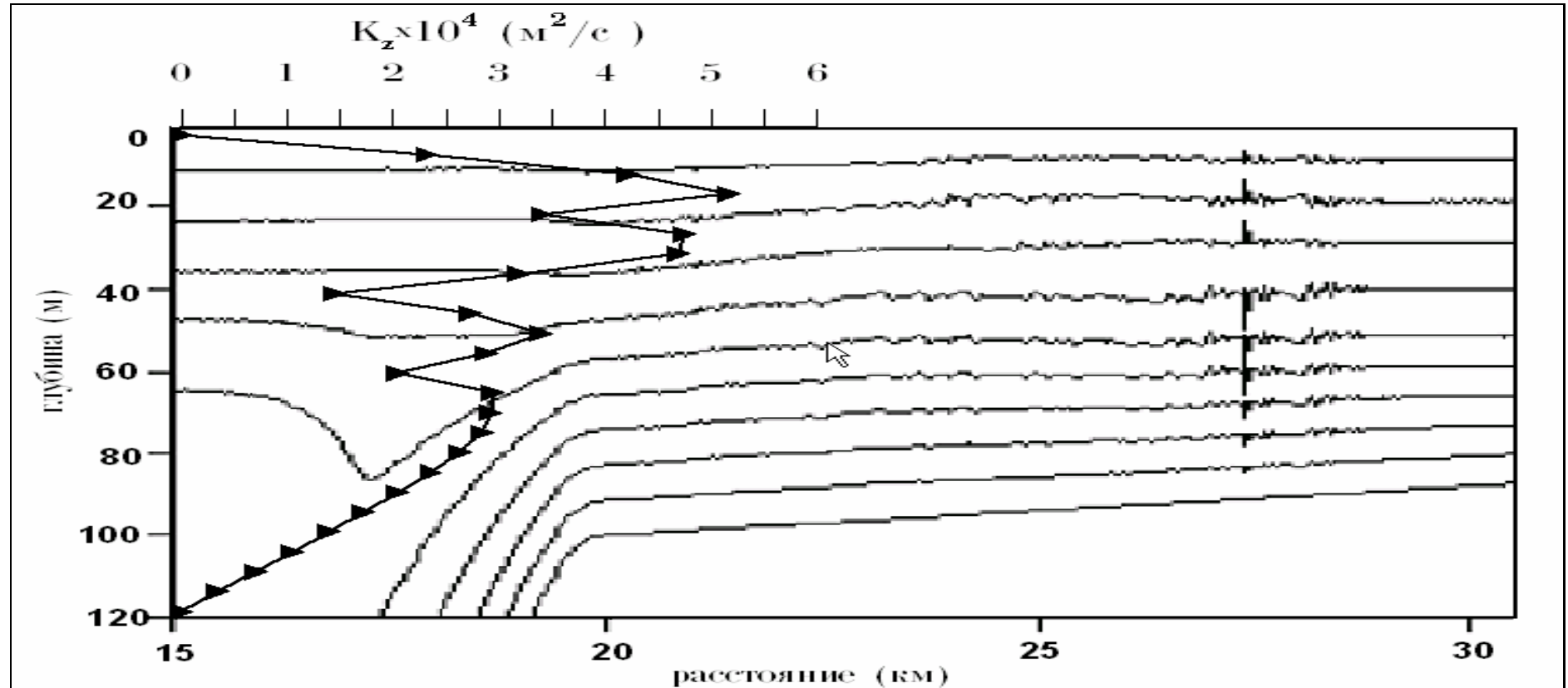
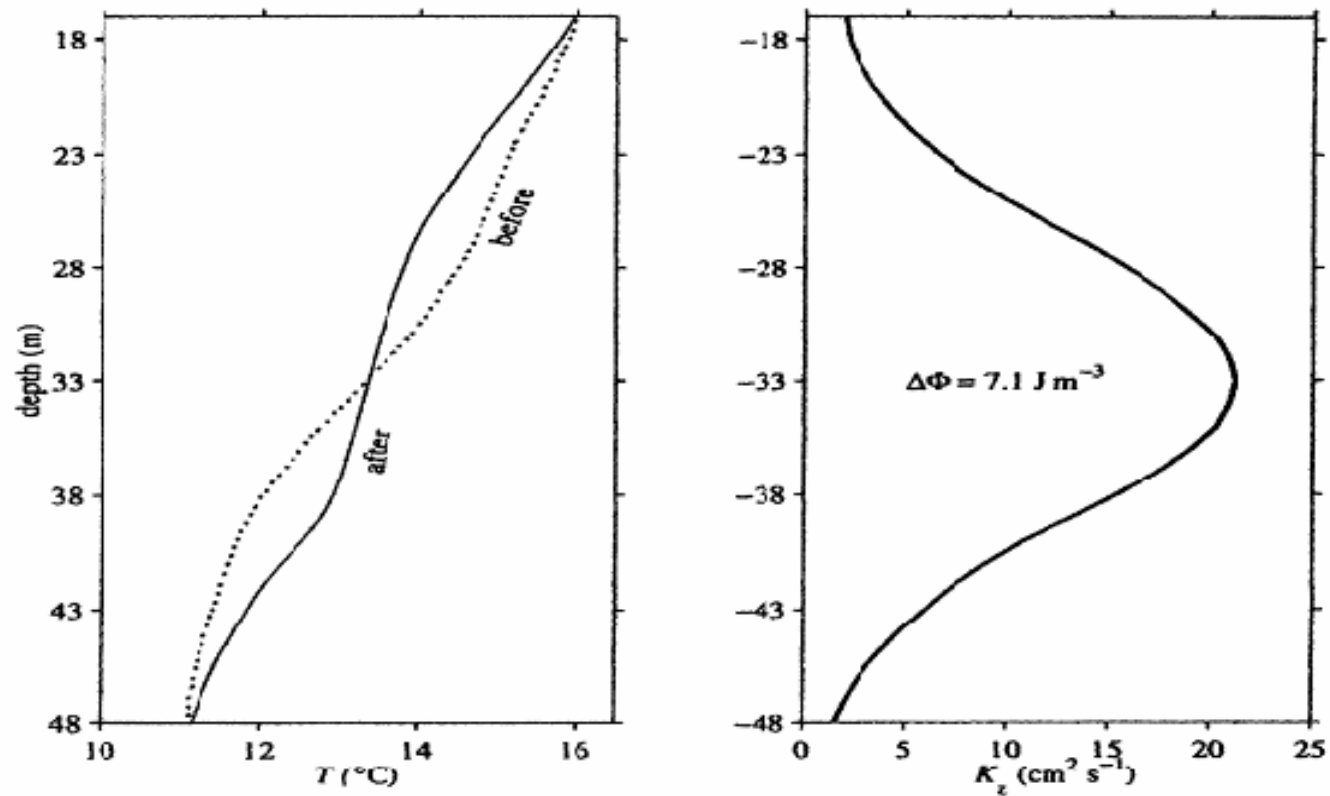


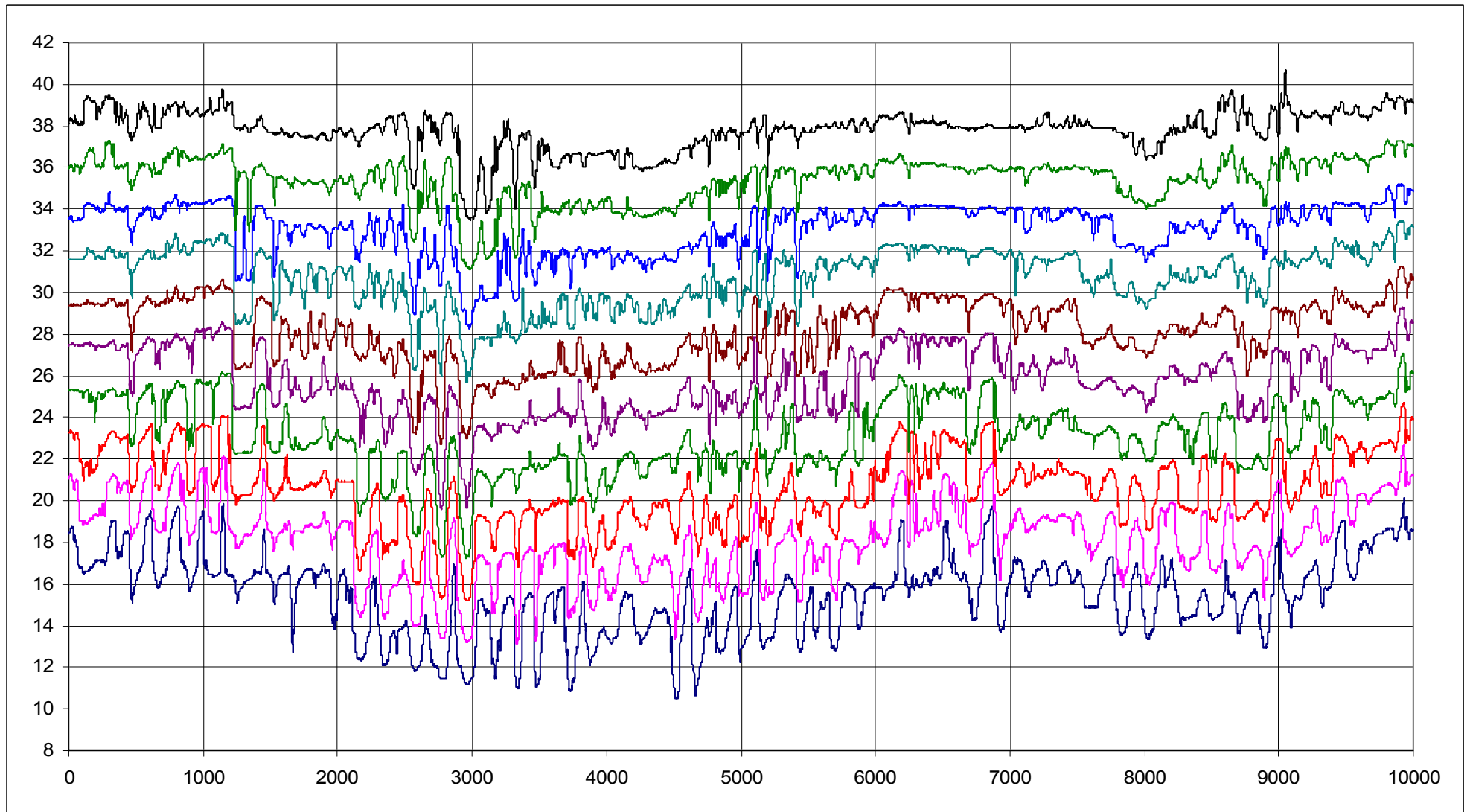
Рис. 4. Вертикальный суммарный коэффициент турбулентного обмена  $K_z$ , рассчитанный у кромки шельфа для осредненного профиля частоты Вяйсяля. Профиль  $K_z$  представлен на фоне модельного разреза изопикн, полученного Навроцким и др. (2003).

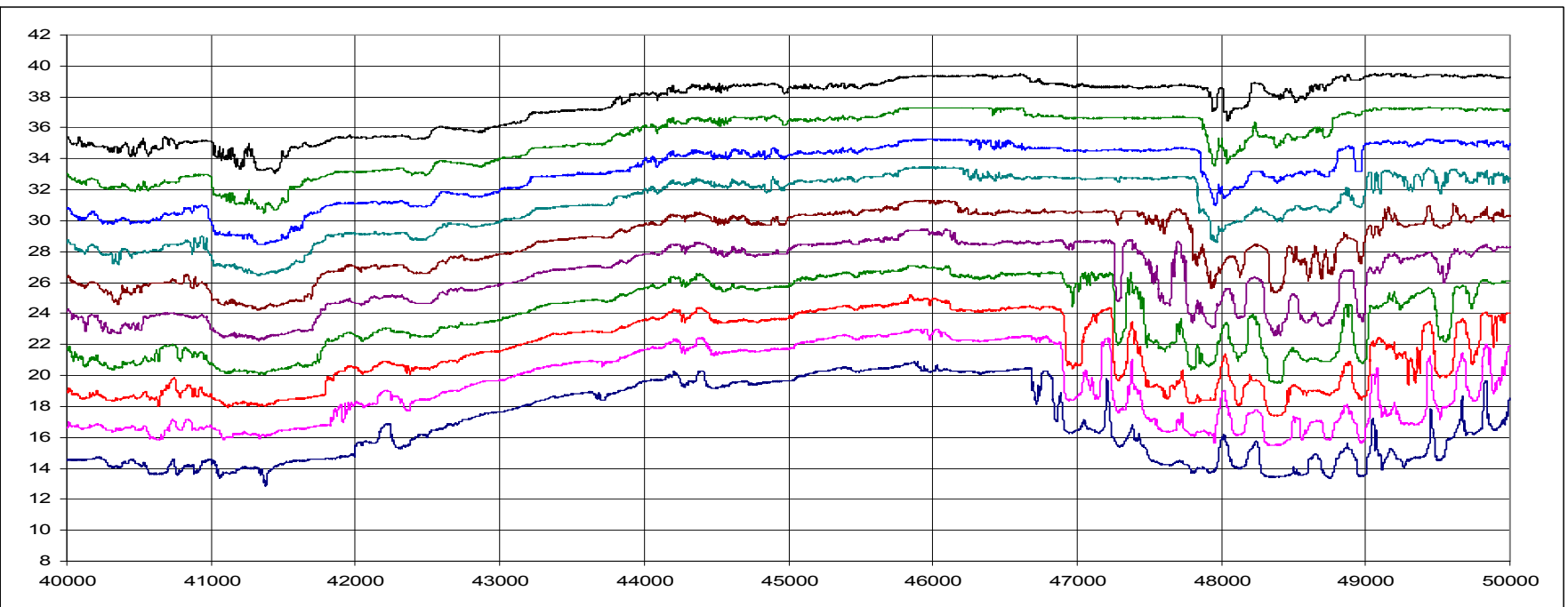
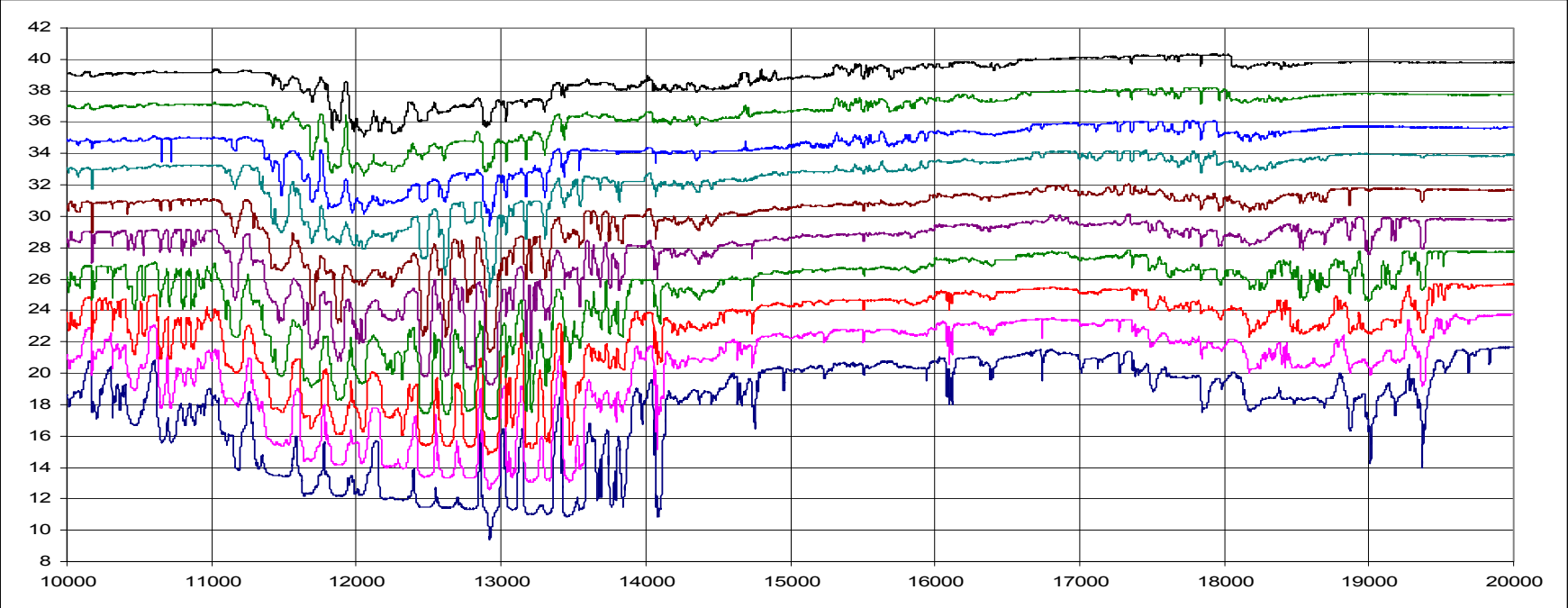
# Inall et al. 2000



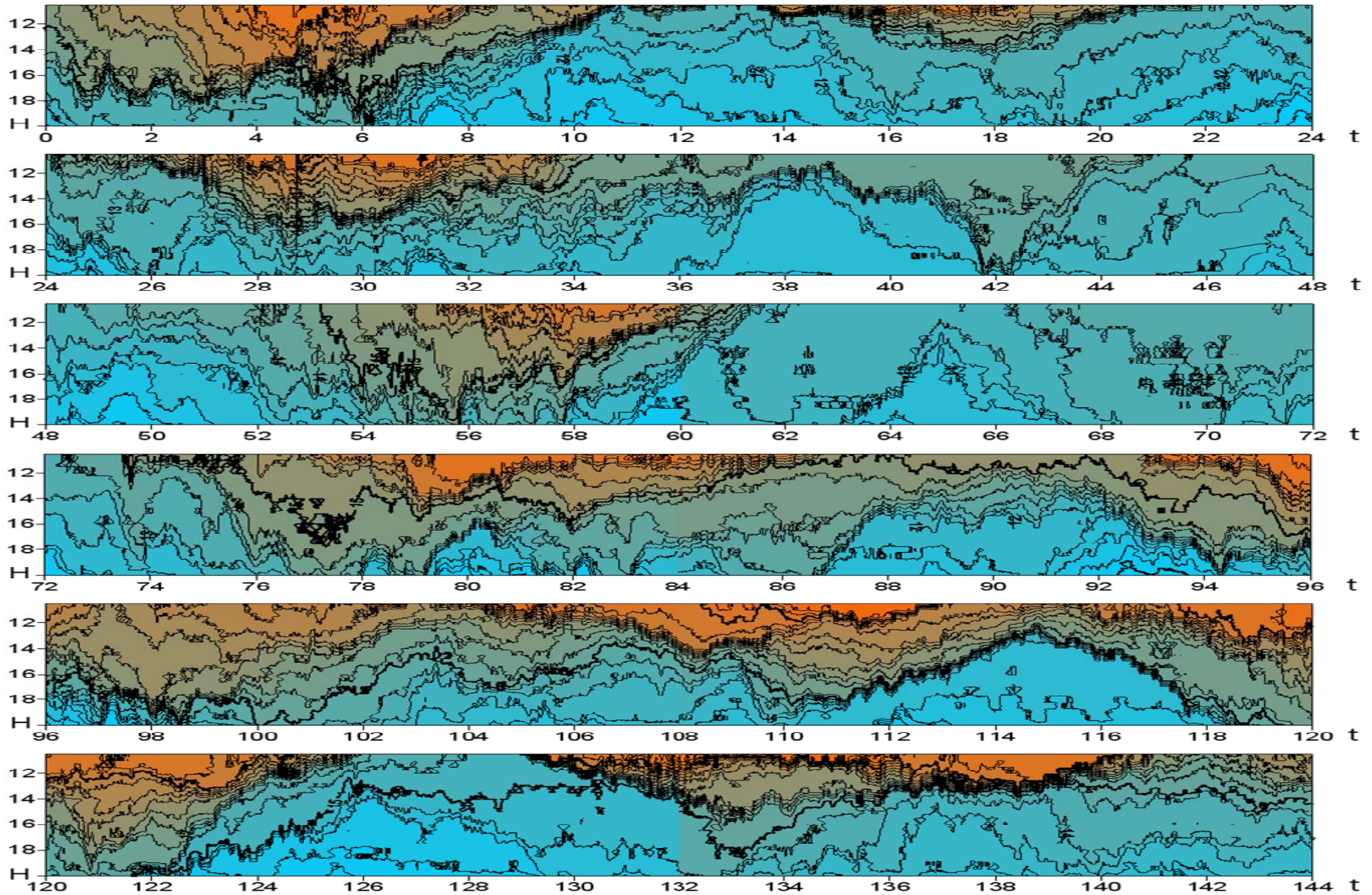
**Figure 12.** Mean temperature profiles before and after passage of packet of NIWs.  $K_z$  as a function of  $z$  calculated from the diffusion equation (see text for details).

# Temperature fluctuations at 10 levels in the near-bottom thermocline

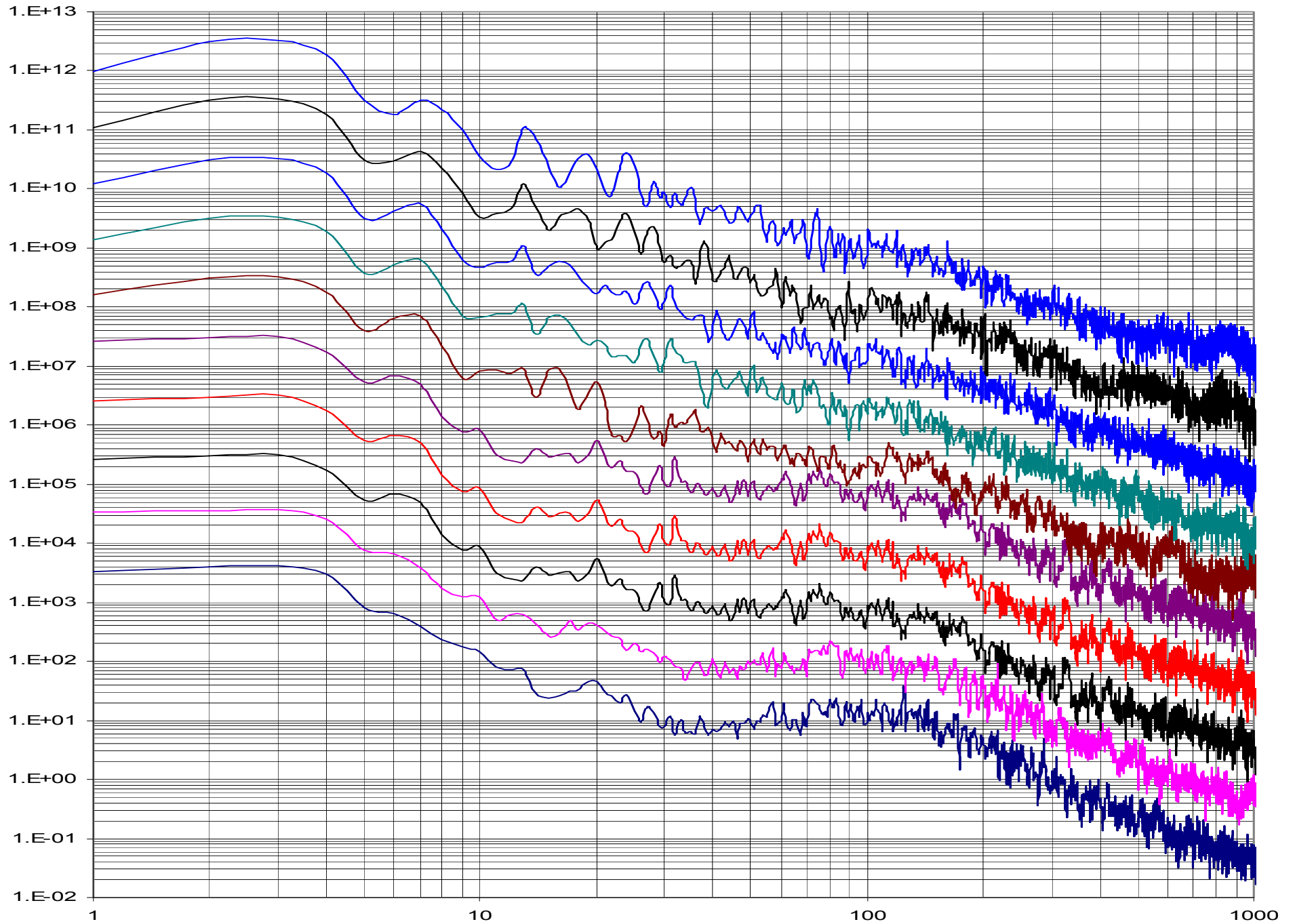


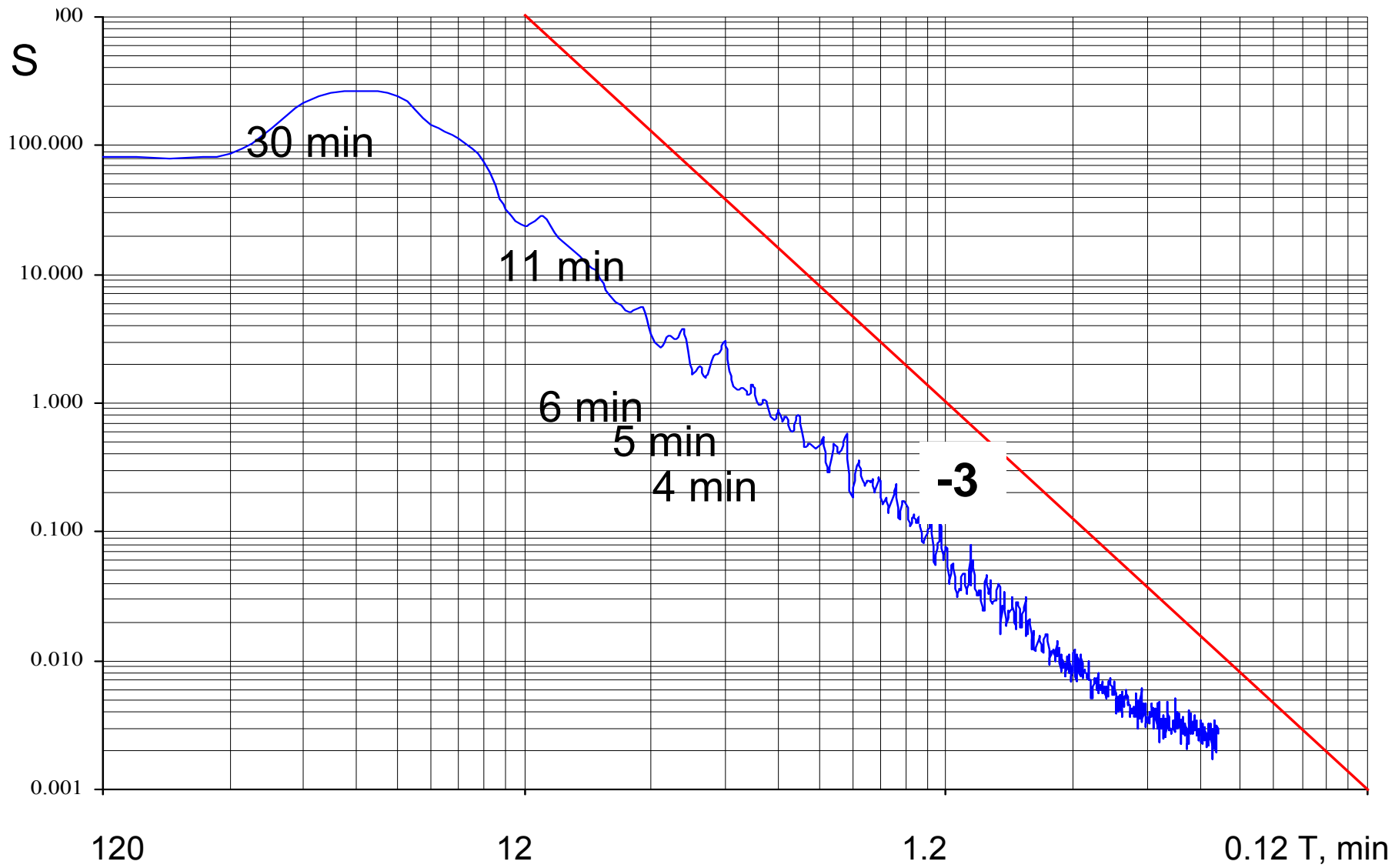


# Temperature fluctuations in fixed points (garlands of sensors)



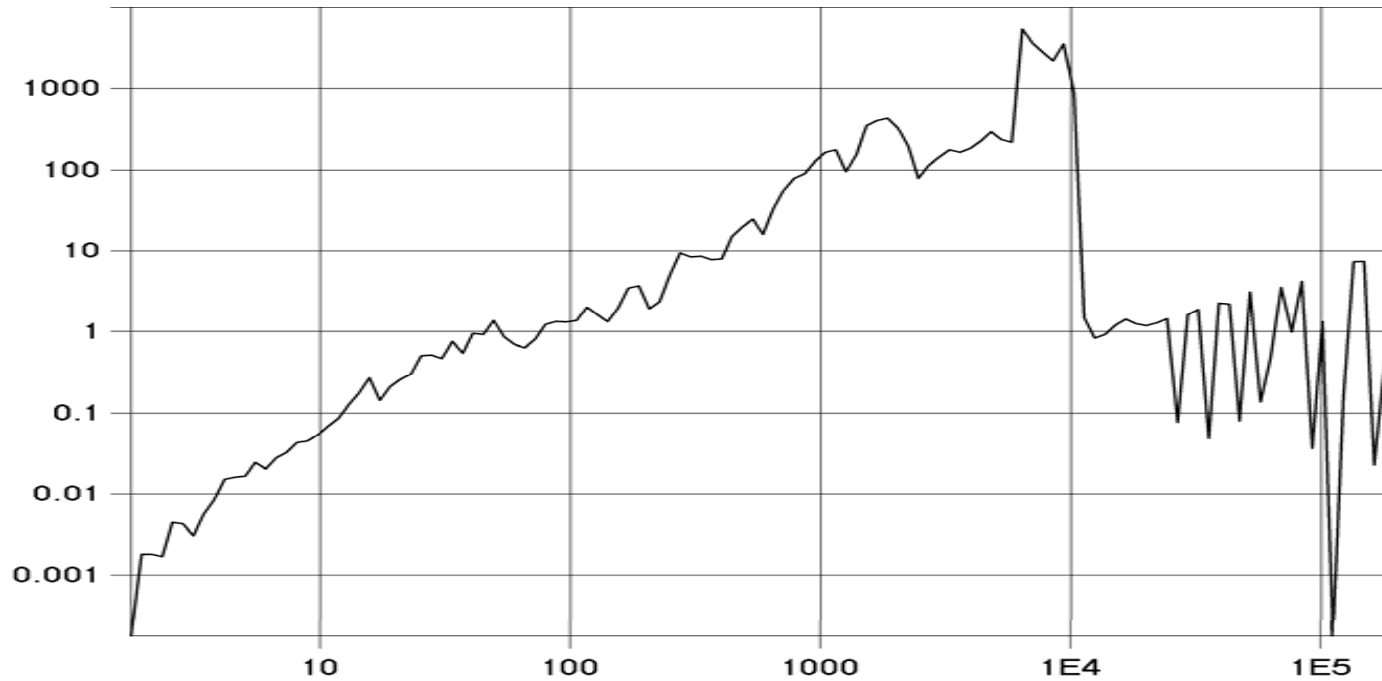
**Temperature fluctuation spectra at 10 levels in the near-bottom layer  
12 - 16.5 m (average of 9 spectra calculated from 48-hours series)**



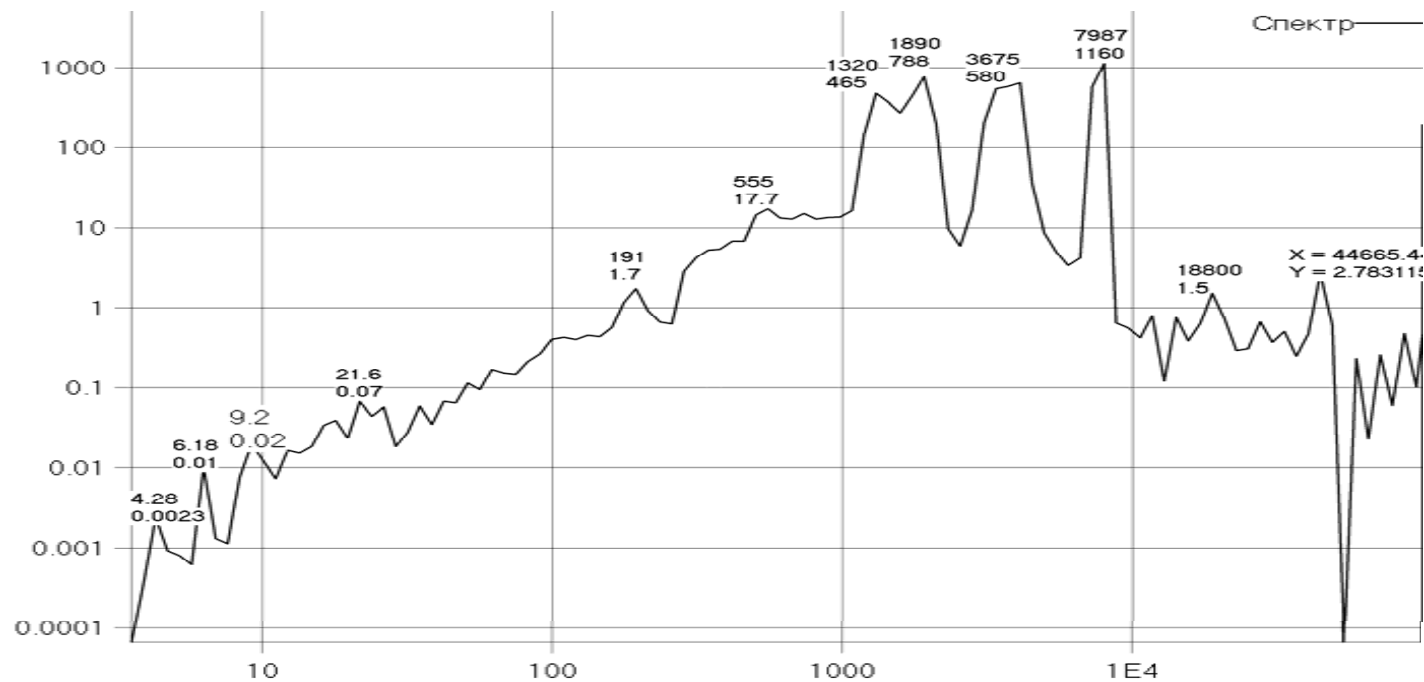


Averaged spectrum of temperature fluctuations in the near-bottom layer

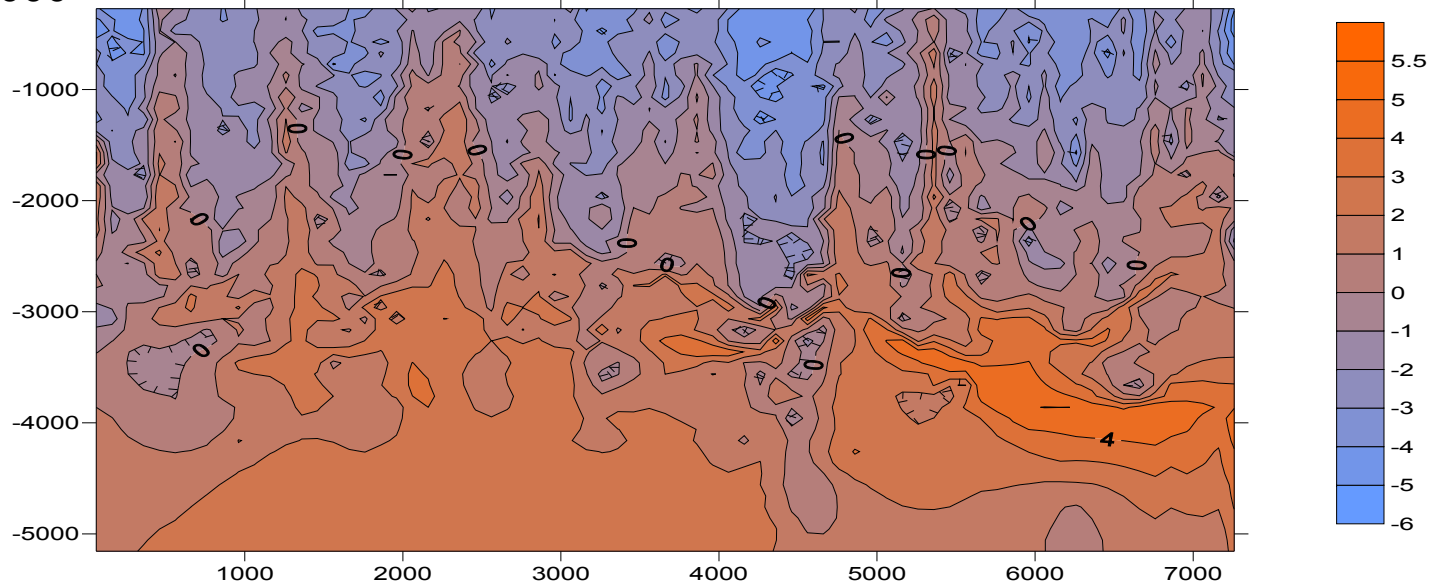
Spectrum of temperature fluctuations at 12 m (August 2006)



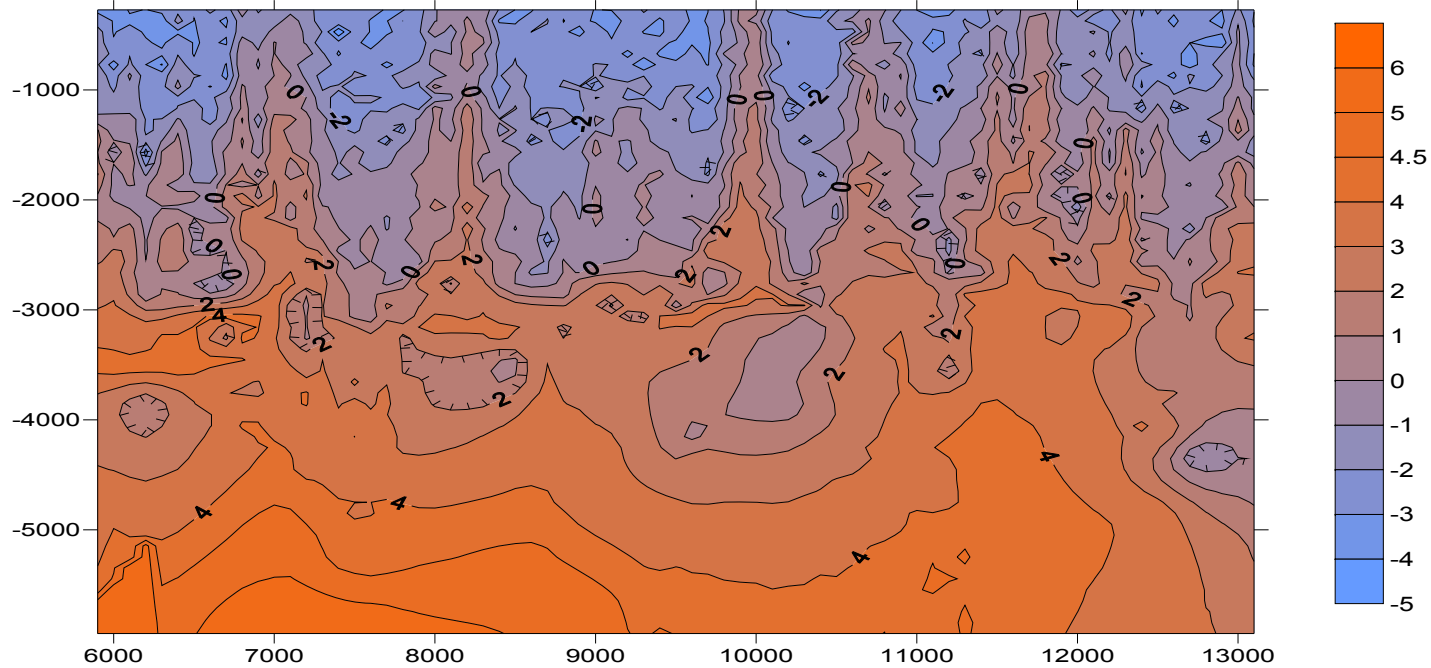
Spectrum of temperature fluctuations at 16 m (August 2006)



$\log F * 1000$

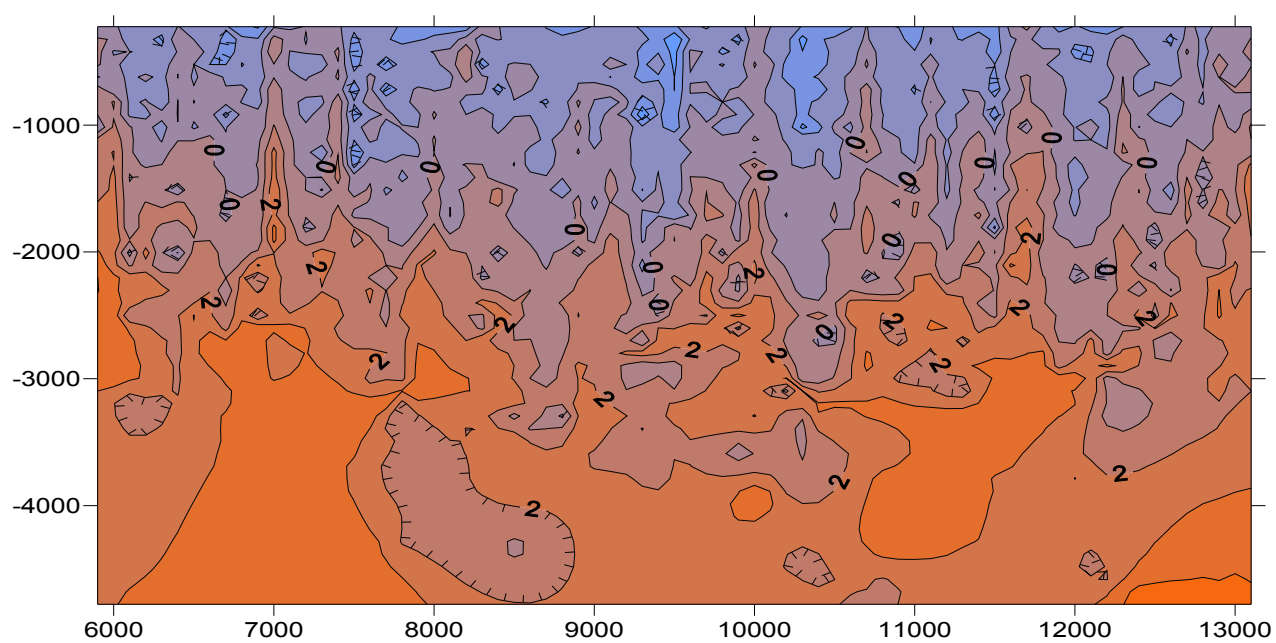
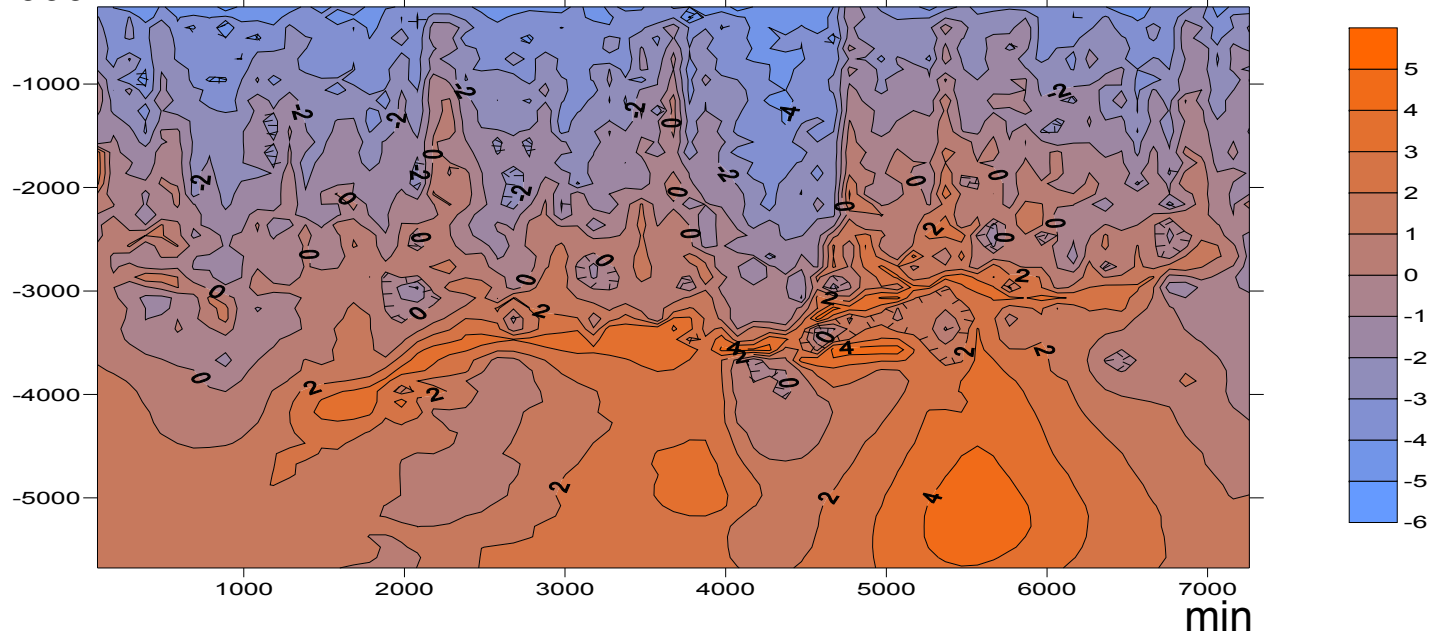


min



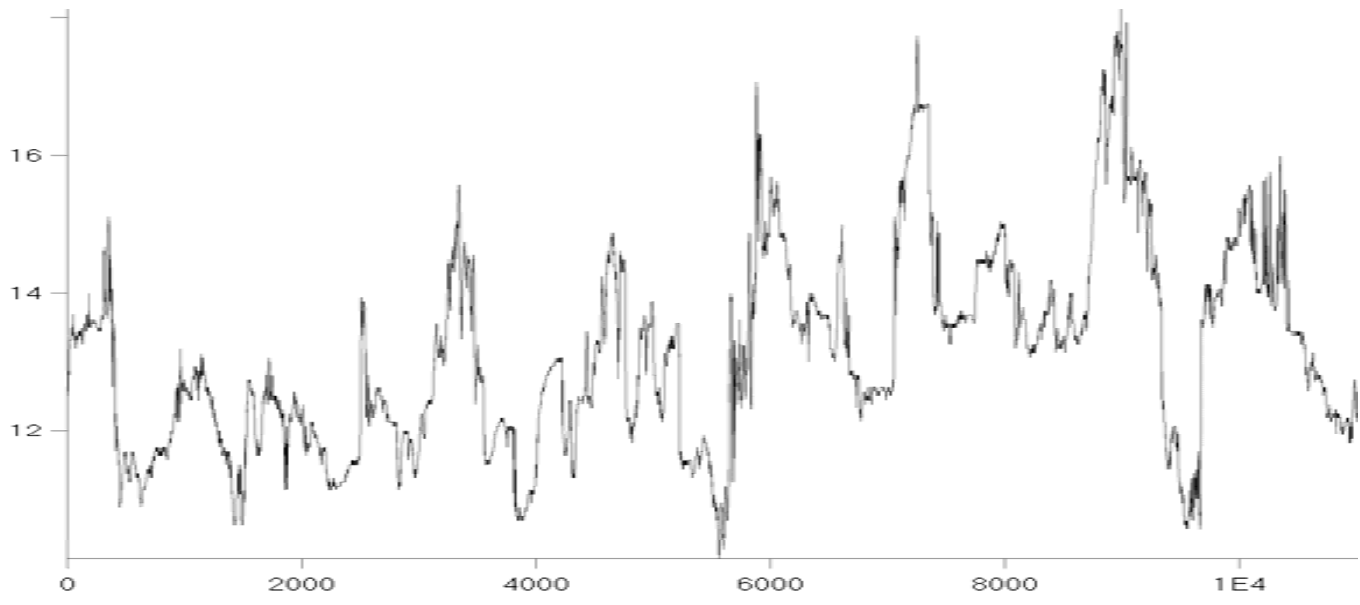
Time-frequency structure of temperature fluctuations at 12 m level in Aug-Sept 2006

logF\*1000



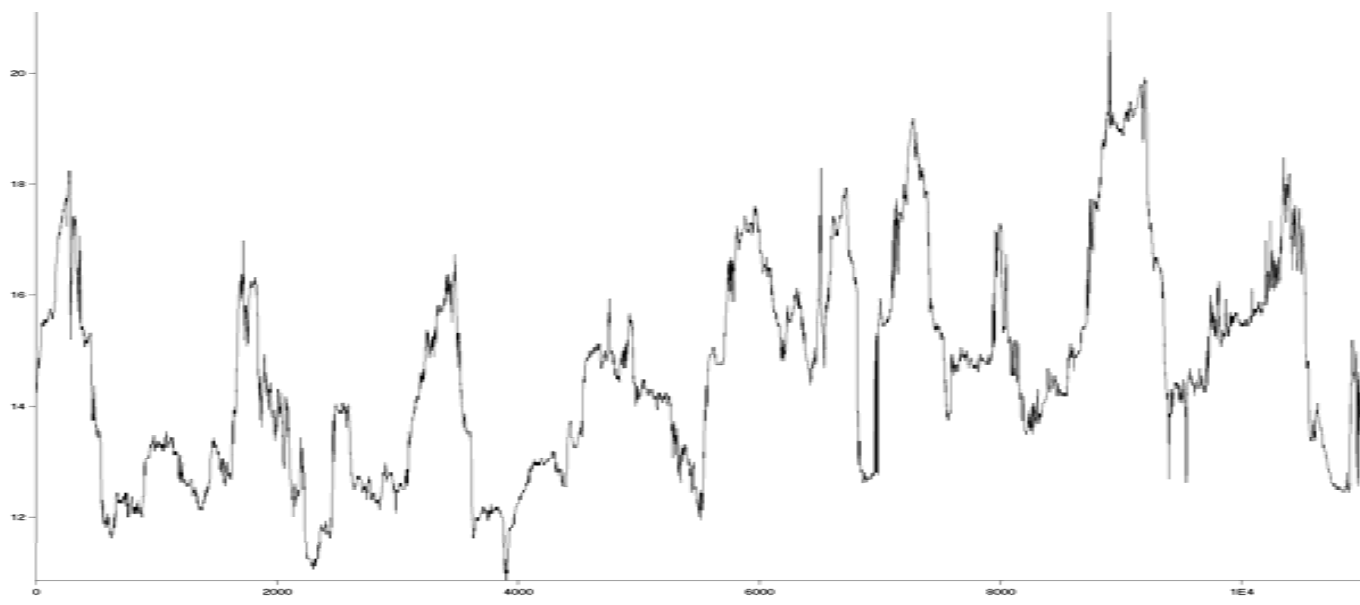
Time-frequency structure of temperature fluctuations at 16 m level in Aug-Sept 2006

T



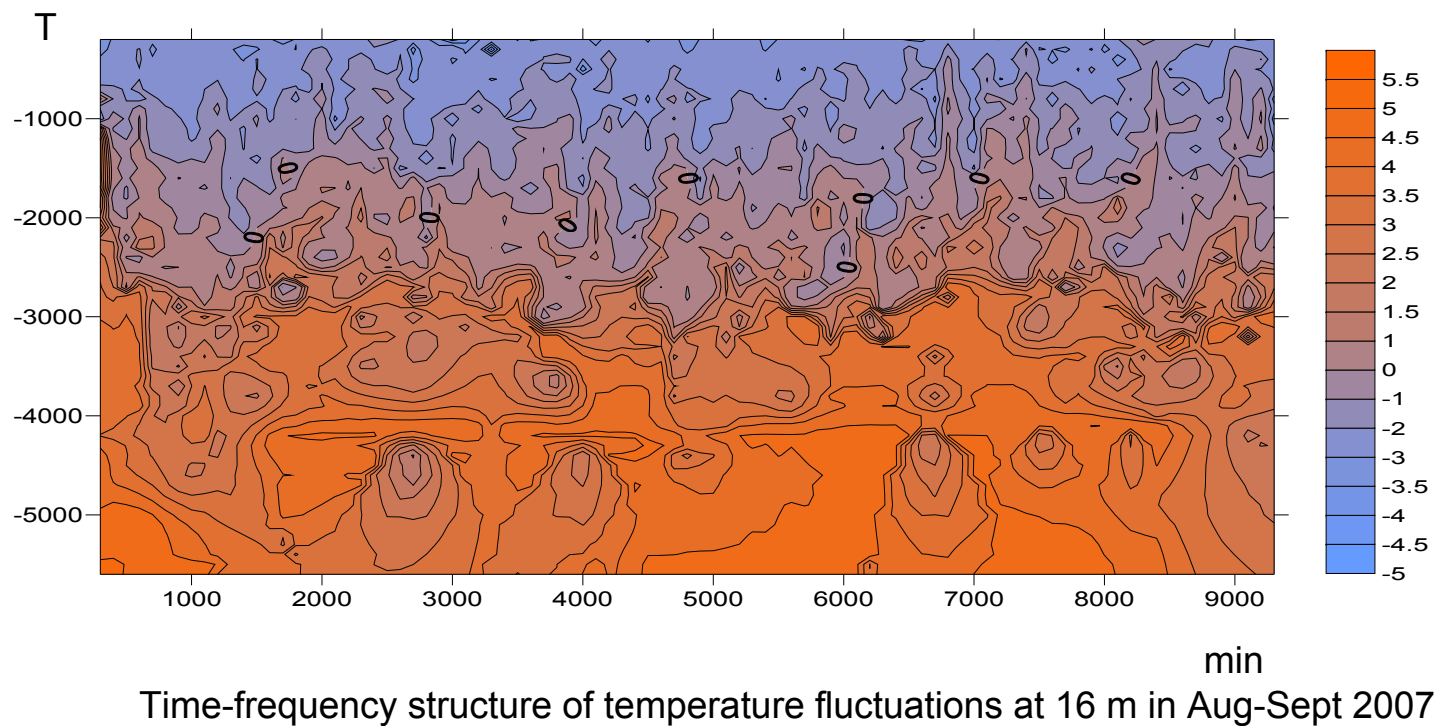
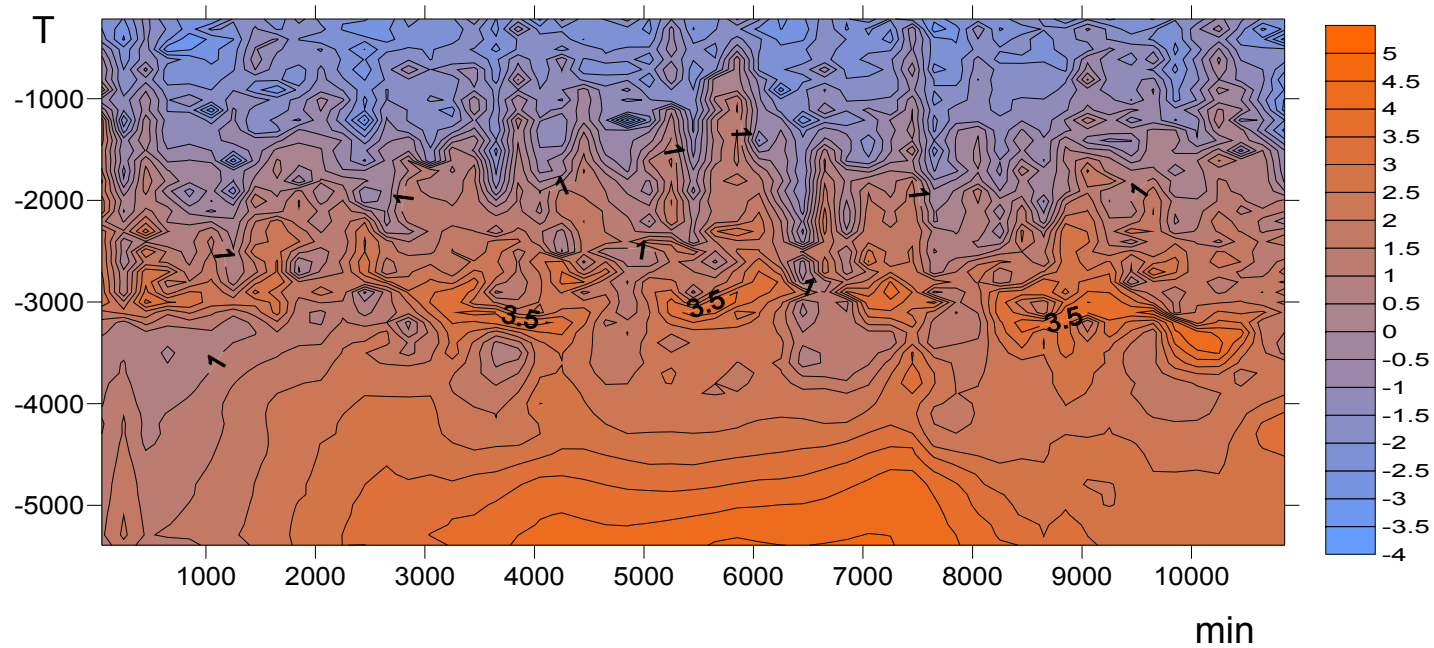
min

Temperature fluctuations at 12 m (August 2007)

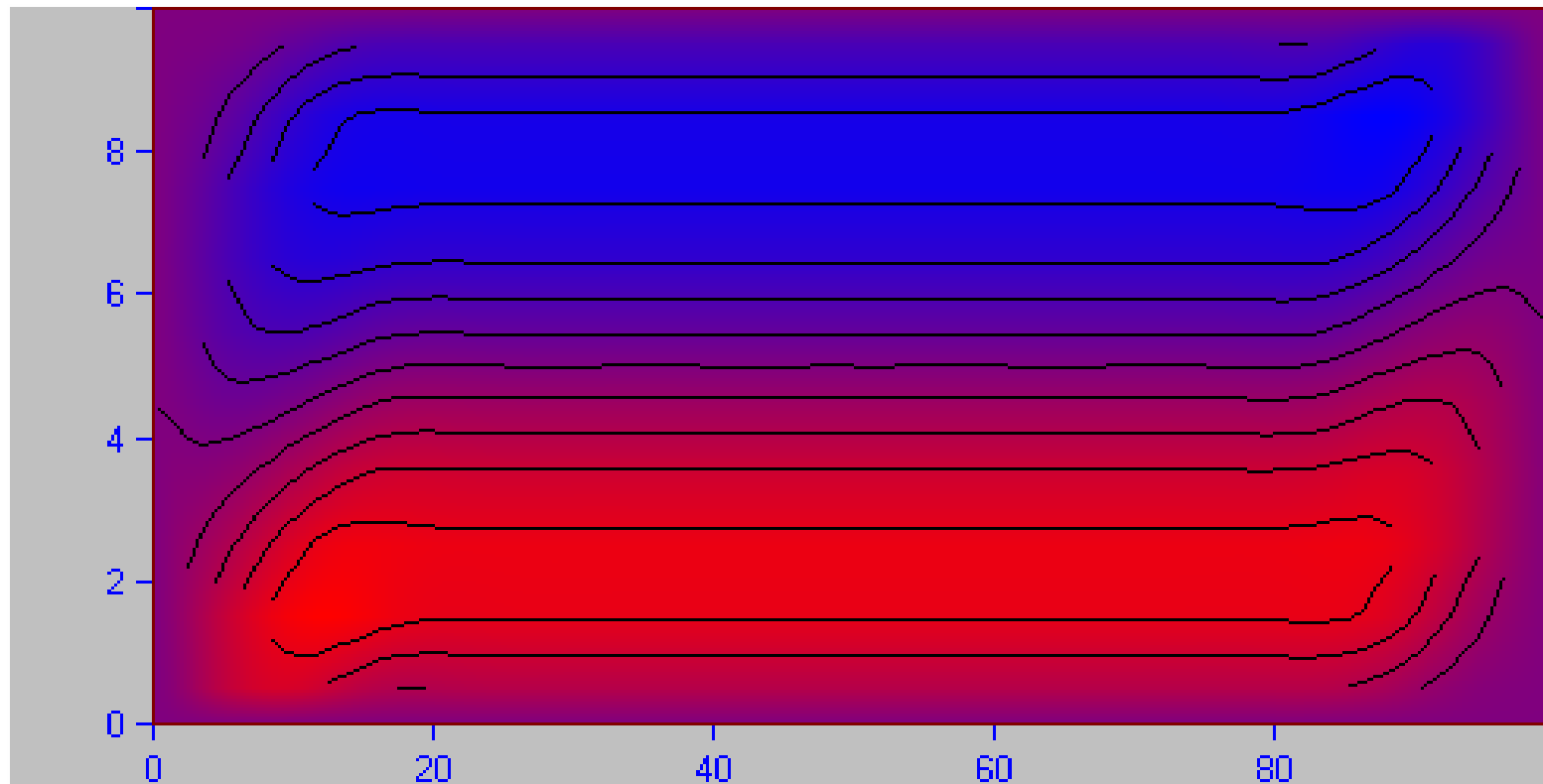


min

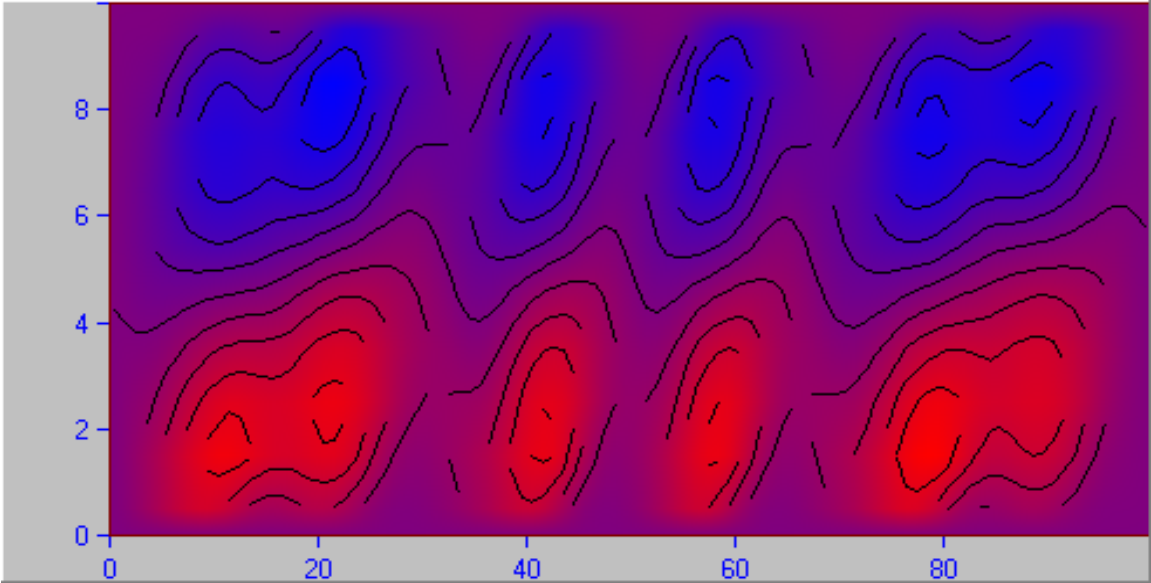
Temperature fluctuations at 16 m (August 2007)



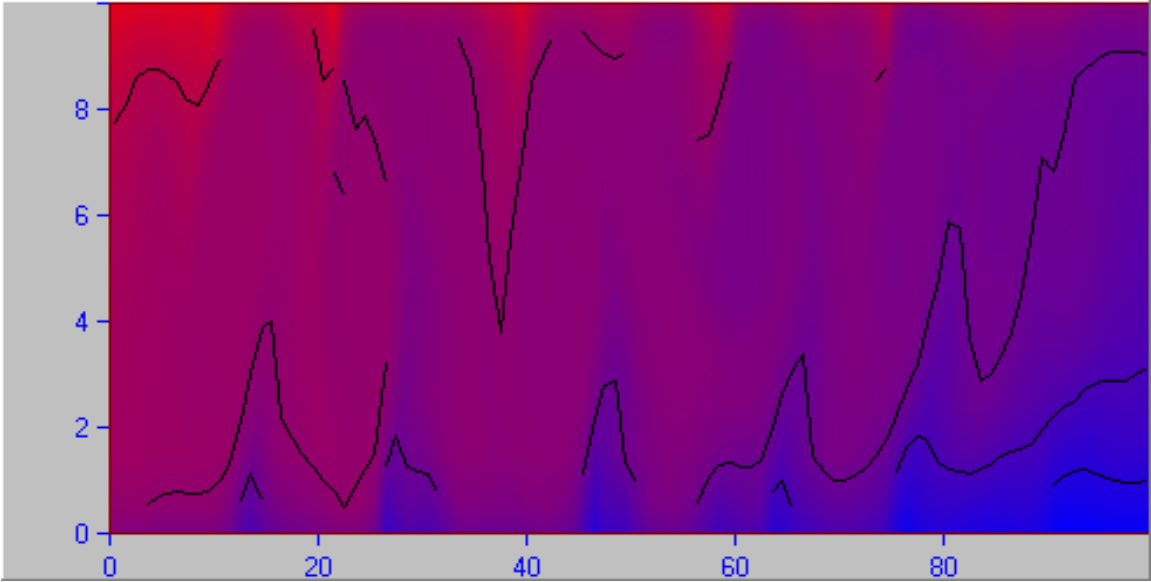
# Low velocity, high viscosity



# Higher velocity

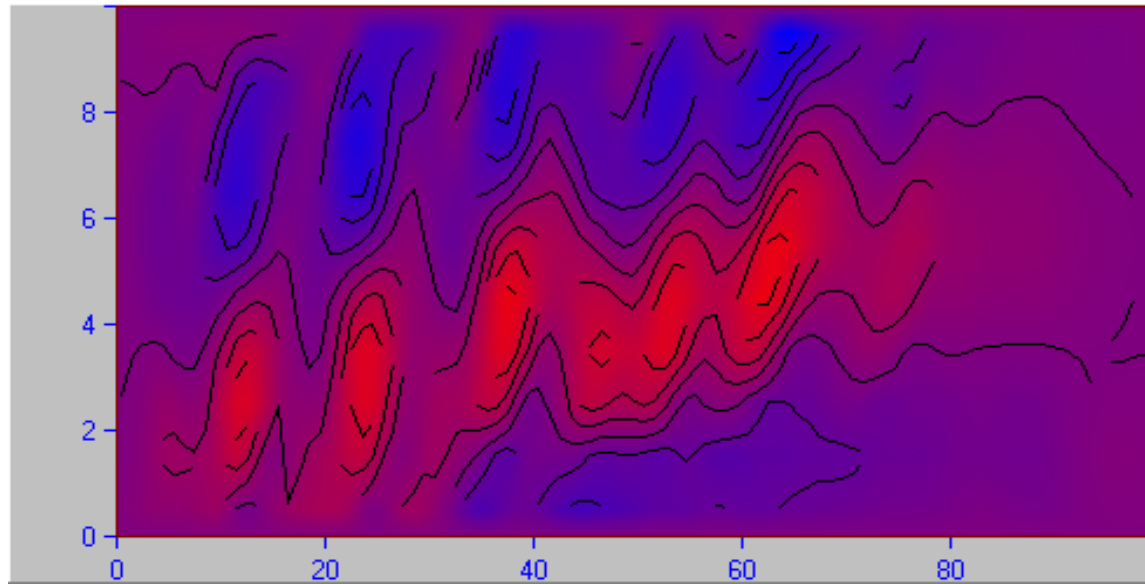


Velocity field

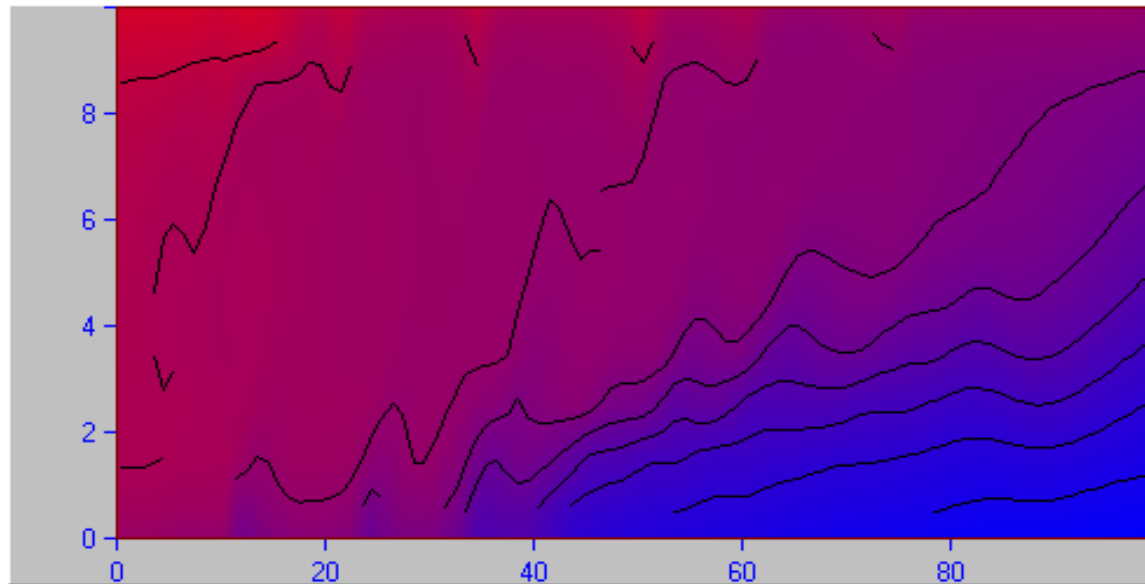


Temperature field

# High velocity



Velocity field



Temperature field

# CONCLUSIONS

**IW lead to considerable mixing in stratified layers and changes in vertical structure of hydrophysical characteristics**

**IW lead to vertical and horizontal fine structure formation, and both of them – IW and FS – are very important for hydroacoustics**

**Internal mixing produced by IW is one of the most important factors of bioproductivity, and it is especially important as a mechanism of effective control of the harmful effects of pollution in shelf zones**

**IW on a sloping bottom lead to intense turbulence generation, specific structure of near-bottom currents and horizontal and vertical transport of different matter**